Peroxiredoxin 4 improved aging-related delayed wound healing in mice

Journal:	*Journal of Investigative Dermatology*
Manuscript ID	JID-2020-1042.R1
Article Type:	Original Article
Date Submitted by the Author:	n/a
Complete List of Authors:	Yamaguchi, Reimon; Kanazawa Medical University, Dermatology 郭, 新; Kanazawa Medical University, Pathology and Laboratory Medicine Zheng, Jianbo; Kanazawa Medical University, Pathology and Laboratory Medicine Zhang, Jing; Kanazawa Medical University, Pathology and Laboratory Medicine Han, Jia; Kanazawa Medical University, Pathology and Laboratory Medicine Shioya, Akihiro; Kanazawa Medical University, Pathology and Laboratory Medicine Uramoto, Hidetaka; Kanazawa Medical University, Thoracic Surgery Mochizuki, Takashi; Kanazawa Medical University, Dermatology Yamada, Sohsuke; Kanazawa Medical University, Pathology and Laboratory Medicine
Keywords:	Aging, Wound Healing, Models, Mouse, Inflammation

Response to the Editor

Editor comments: The authors should adequately respond to all of the comments below and revise the submission accordingly. Although additional supporting data is necessary, experiments involving wounding of tail skin are not anticipated,

Section/Deputy Editor: 1

Comments to the Author:

This manuscript focuses on the role of Peroxiredoxin 4 (PRDX4) in the control of wound healing in mice by using multiple genetic mouse models including PRDX4 transgenic and knockout mice. The authors conclude that PRDX4 may be beneficial for wound healing process because it regulates multiple important mechanisms including proliferation and migration of fibroblasts, increases fibroblast resistance to oxidative stress, and inhibits wound-associated skin inflammation. However, the reviewers find that there are issues that need to be addressed. Although one reviewer suggests additional wound model to validate wound closure data (tail wound model) given the proposed mechanism of action this additional work would be only reinforcing the conclusions. For other specific comments of the reviewers please see their individual comments below.

Response:

In accordance with the Reviewers' & Editor's kind and constructive suggestions, we extensively revised our manuscript (Ms ID # JID-2020-1042) entitled R1 "Peroxiredoxin 4 improved aging-related delayed wound healing in mice". The following changes were implemented:

1. Added data related to hyperproliferative epithelium and collagenous ECM.
2. Provided information on PRDX4 variation mice.
3. Changed the confusing pictures.
4. Rewrote the Discussion section, to make it more concise (it was shortened by

approximately 25%).

The comments were very helpful for revising and improving our paper, and provided important guidance in relation to our future study. Our specific responses to the reviewers' comments, as well as the changes made to the manuscript are provided below. Changes made to the manuscript in response to the reviewers' comments are indicated with underlining and bold typeface. We hope that the revised manuscript is now suitable for publication in your journal.

Reviewer comments:

Reviewer: 1

Comments to the Author

Major concern:

The authors claimed that PRDX4 is essential and functions as a key molecule in mouse skin wound healing. This reviewer feels that the data presented in this manuscript are not convincing enough to support the authors' conclusion.

Response:

At first, we would like to express our thanks to the reviewer for his or her efforts in improving this manuscript. In this study, we subjected PRDX4 transgenic and knockout mice of three age groups (young, adult, and aged) to skin wound formation, and observed the changes in wound healing in these mice within 7 days. Based on the *in vivo* results, we focused on the role of PRDX4 in fibroblasts. Therefore, by harvesting fibroblasts from the normal skin of these mice, we also investigated the effect of PRDX4 on fibroblast behavior *in vitro*. We think that these *in vivo* and *in vitro* results should support the conclusion that PRDX4, at least within 7 days, should be a key molecule in mouse skin wound healing. Even so, in the revised manuscript, we added the results related to hyperproliferative epithelium and collagenous ECM and provided the data on these variations of the mice phenotype. We believe, given these additional results, that the data in this study should be sufficient to support our conclusion. Thank you so much for your help in improving our manuscript.

Other concerns:

Need more detailed information of PRDX4 knockout (PRDX4$^{-/y}$) and hPRDX4 transgenic (hPRDX4$^{+/+}$) mice, such as skin phenotype and also generation of these mice. Are these mice cell-type specific? Are there any phenotypic changes in skin dermis in these mice? Such information is very useful as the authors emphasized dermal fibroblasts.

Response:

Thank you very much for your valuable suggestions. According to the reviewer's suggestion, we have added a description about the generation of *PRDX4*$^{-/y}$ and *hPRDX4*$^{+/+}$ mice to the 'Animals' section in 'SUPPLEMENTARY MATERIALS AND METHODS'. In addition, the data related to skin phenotype of these mice are shown below and have been added to Supplementary figure S2.

PRDX4$^{-/y}$ and *hPRDX4*$^{+/+}$ mice are not cell-specific, but hPRDX4 is significantly expressed in the fibroblasts of transgenic mice. Based on our additional results, no phenotypic changes were observed in the skin dermis of *PRDX4*$^{-/y}$ and *hPRDX4*$^{+/+}$ mice, in comparison to WT mice. We have added some contents about the construction of *PRDX4*$^{-/y}$ and *hPRDX4* $^{+/+}$ mice into the 'Animals' section of the 'SUPPLEMENTARY MATERIALS AND METHODS', as follows:

The primers for hPRDX4 were designed based on a published sequence (Genebank accession no. NM_006406). hPRDX4 cDNA was amplified by reverse transcription–polymerase chain reaction and cloned into the pGEM-T easy vector

system (Invitrogen, Life Technologies Japan Ltd., Tokyo, Japan) (Supplementary Figure S1a) (Guo et al., 2019, Guo et al., 2012, Yamada et al., 2012, Meier et al., 1996). The NotI fragment containing hPRDX4 cDNA was inserted into the NotI site of pcDNA3 (5.4 kb; Invitrogen, Life Technologies Japan Ltd.), and a bovine growth hormone polyadenylation (BGHPA) sequence was inserted into the tail of the transgene to stabilize the expression. The entire nucleic acid sequence, containing a 0.6-kb cytomegalovirus (CMV) enhancer/promoter, the 0.8-kb hPRDX4 cDNA, and the 0.2-kb BGHPA sequence, was purified by restriction enzyme digestion with BglII and SmaI, and was microinjected into the male pronuclei of one-cell C57BL/6 mouse embryos using standard transgenic techniques to generate transgenic mice. The *PRDX4* $^{-/y}$ mice were previously generated by Fujii et al (Iuchi et al., 2009) by cloning and sequencing mPRDX4 genomic DNA from a b129/SVJ mouse genomic library (Stratagene), and constructing a targeting vector using the cloned DNA fragment. As the chimeric male mice generated from the embryonic stem cells were infertile, they performed intracytosolic sperm injection into blastocysts and implanted them into the uteri of pseudopregnant C57BL/6 female mice.

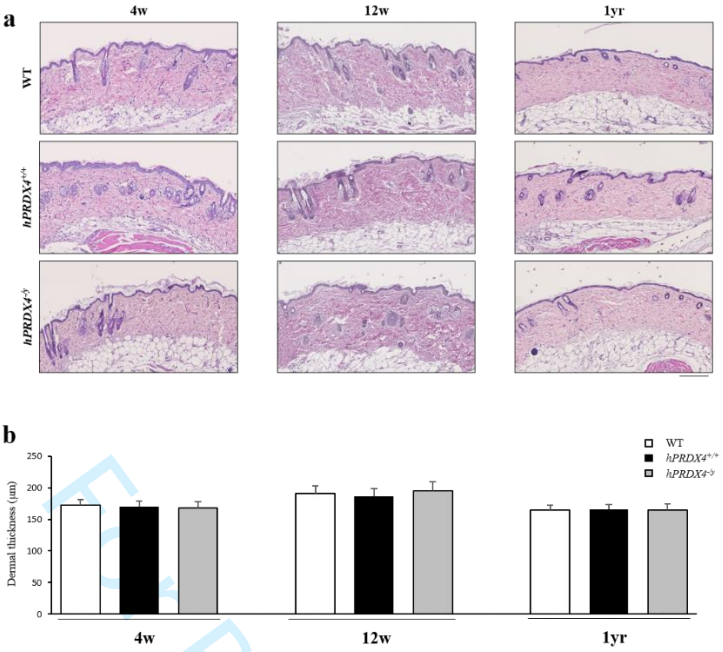

Is there any change in collagenous ECM in these mice before and after wound?

We additionally investigated the expression of collagen I and III in the normal and wound skin tissue of these mice, and found that the expression levels did not differ to a statistically significant extent among the three groups. The results were shown below and have been added to Supplementary Figure S6. PRDX4—at least in the inflammatory phase and early proliferative phase—may not play important roles in collagenous ECM production during wound healing. Collagenous ECM production is more important for wound healing in the later proliferative phase and remodeling phase. Thus, because we only observed the results within 7 days, we cannot deny an association between PRDX4 and collagenous ECM. However, we consider that to be beyond the scope of the present study, the subject about collagenous ECM will be further investigated in a future study.

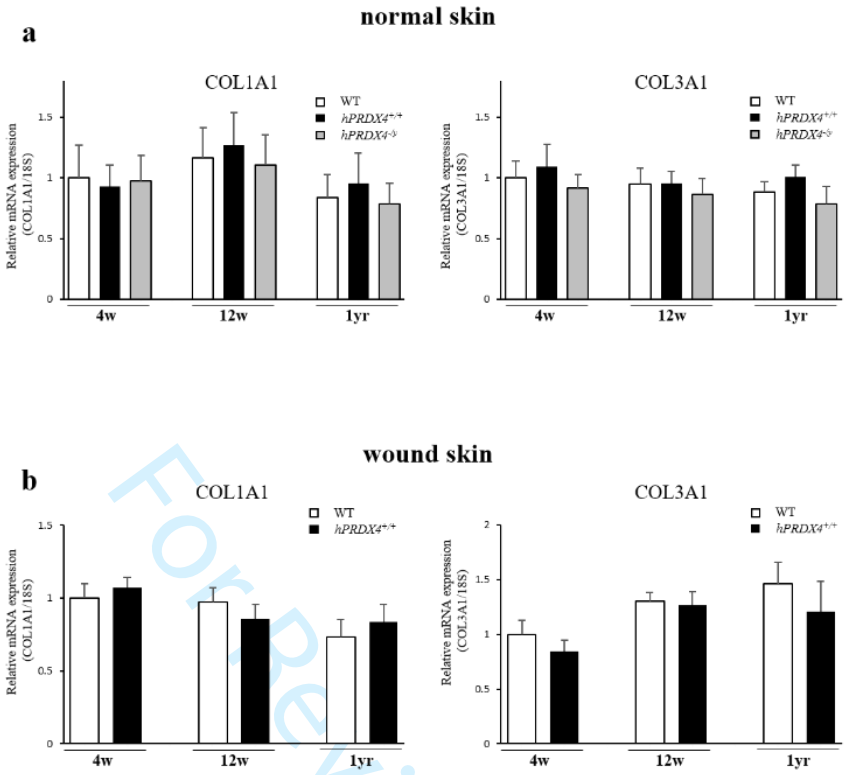

Fig 4a, 4b a-SMA staining is not convincing. Obviously, mouse dorsal skin wound is very different than human skin wound, mouse wound healing is largely controlled by contraction through a-SMA positive cells, as human skin wound healing involves granulation tissue formation and re-epithelialization. The authors may need to try wound from mouse tail, which is more relevant to human skin wound.

Response:

We thank the reviewer for their constructive suggestion. For the following reasons, a tail wound model may not be necessary for this study. Firstly, as the reviewer says, the mechanism of wound healing differs between humans and mice. However, fibroblasts/myofibroblasts play an important role in these two different mechanisms. In humans, the main cellular component of granulation tissue is also fibroblasts/myofibroblasts, and faster and better granulation tissue formation is also very helpful for wound healing. In this study, we focused on the role of PRDX4 in fibroblasts/myofibroblasts and found that PRDX4 can promote the proliferation and migration of fibroblasts/myofibroblasts to accelerate wound healing. Thus, PRDX4 may potentially have a similar effect in humans. Of course, that needs to be further investigated in a future study. Secondly, the model used in the present study is a widely accepted and used mouse model for the study of wound healing, which is also applied in many studies on re-epithelialization, angiogenesis, and the fibroblast function during wound healing[1-3]. Thirdly, it has also been reported that even in simple full-thickness skin wound models, the early stage of wound healing in mice is very close to the human mechanism and is

sufficiently reproducible[4]. Finally, tail tissue is also mouse tissue and there are still many aspects of wound healing that are different from human wound healing. The process of wound healing in the tail is closer to the healing of skin tissue in other parts of mice, in comparison to that in humans.

Ref.

1) Uchiyama A, Nayak S, Graf R, Cross M, Hasneen K, Gutkind JS, et al. SOX2 Epidermal Overexpression Promotes Cutaneous Wound Healing via Activation of EGFR/MEK/ERK Signaling Mediated by EGFR Ligands. J Invest Dermatol. 2019;139:1809-20.e8.

2) Ishida Y, Kuninaka Y, Nosaka M, Furuta M, Kimura A, Taruya A, et al. CCL2-Mediated Reversal of Impaired Skin Wound Healing in Diabetic Mice by Normalization of Neovascularization and Collagen Accumulation. J Invest Dermatol. 2019;139:2517-27.e5.

3) Laplante P, Brillant-Marquis F, Brissette MJ, Joannette-Pilon B, Cayrol R, Kokta V, et al. MFG-E8 Reprogramming of Macrophages Promotes Wound Healing by Increased bFGF Production and Fibroblast Functions. J Invest Dermatol. 2017;137:2005-13.

4) Chen L, Mirza R, Kwon Y, DiPietro LA, Koh TJ. The murine excisional wound model: contraction revisited. Wound Repair Regen. 2015;23:874-7

The authors described the mice used in this study are C57BL/6 background. Why the mice show white hair?

Response:

It may be just a visual deviation. The whitish skin after shaving may have interfered with the reviewer's observation. As shown in the photo below, the C57BL/6 background mice that we used had black hair in the WT, *hPRDX4*$^{+/+}$, *PRDX4*$^{-/y}$ groups (all groups), and in all age groups (Figure).

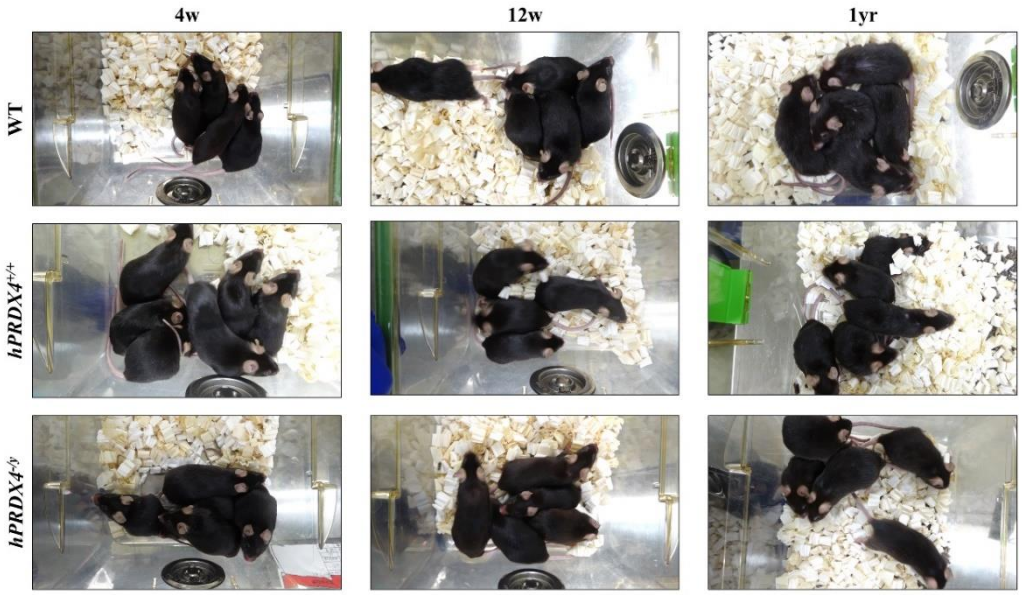

Fig 2A PRDX4 IHC and Western blot are not match, Western shows only minor increased of PRDX4. PRDX4 IHC seems like not true staining, the backgrounds are very different.

Response:

IHC and WB are two different methods for detecting the expression of proteins, and many factors can influence the results of these two experiments, including antigen repair (IHC), protein dosage (WB), the timing of DAB color (IHC) and exposure (WB), and the contrast control of the image. Therefore, two methods are needed to confirm the protein expression. According to the reviewer's suggestion, after adjusting for these influencing factors, we changed the confusing pictures, which makes the results of the two experiments appear more consistent. We apologized that these IHC pictures were analyzed by two software programs, which may have led to the different backgrounds. We used the same software program to readjust these images and provided new pictures. The modified figure (Figure 2a, b) is shown below.

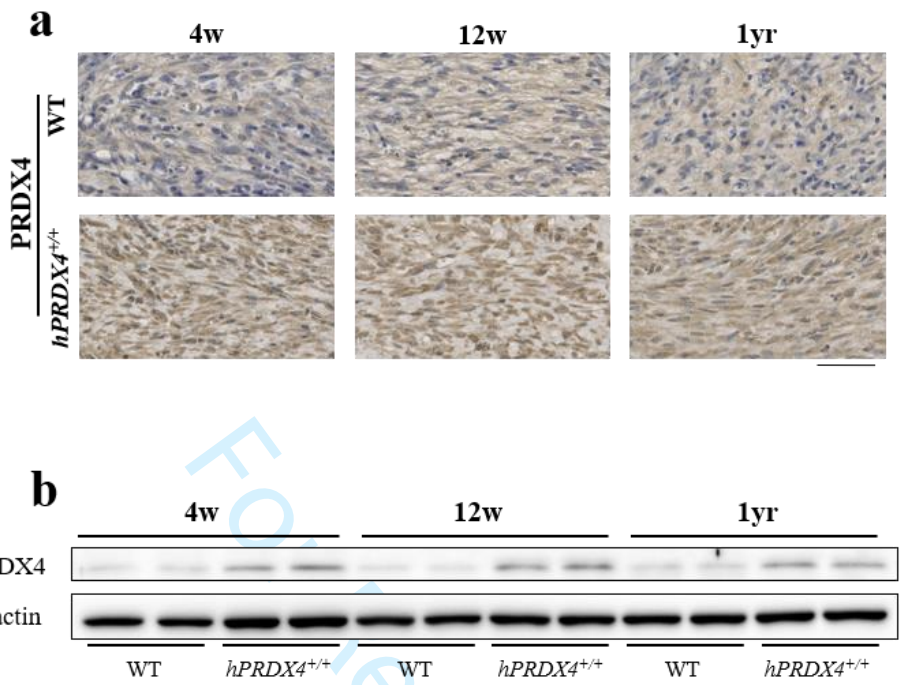

The manuscript is poorly writing and organized. There are rooms for improvement in writing.

Response:

The discussion of this paper may have been too long, which might have made it difficult to follow. We rewrote the Discussion and shortened it by approximately 25%. The revised manuscript should be more concise and clearer for readers. This manuscript was edited again by a professional editor, Brian Quinn (Japan Medical Communication), who is a native speaker of English.

Reviewer: 2

Comments to the Author

In this manuscript, the authors study the role of Peroxiredoxin 4 (PRDX4) in the control of wound healing in mice. A number of genetically engineered mouse models have been used including PRDX4 transgenic and knockout mice. Based on the results presented in the manuscript, the authors conclude that PRDX4 is beneficial for wound healing process and promotes proliferation and migration of fibroblasts, increase their resistance to oxidative stress, and inhibits wound-associated skin inflammation. Overall, the conclusions are based on solid data presented in the manuscript. The only few minor comments need to be addressed.

1. **Please, provide more information here on hPRDX4$^{+/+}$ mice (which kind of promoter has been used, etc.).**

Response:

Thank you for your important suggestions. The design of the hPRDX4 transgene is shown below. We have added some contents about the construction of *hPRDX4* $^{+/+}$ mice into the 'Animals' section of the 'SUPPLEMENTARY MATERIALS AND METHODS', as follows:

The primers for hPRDX4 were designed based on a published sequence (Genebank accession no. NM_006406). hPRDX4 cDNA was amplified by reverse transcription–polymerase chain reaction and cloned into the pGEM-T easy vector system (Invitrogen, Life Technologies Japan Ltd., Tokyo, Japan) (Supplementary Figure S1a) (Guo et al., 2019, Guo et al., 2012, Yamada et al., 2012, Meier et al., 1996). The NotI fragment containing hPRDX4 cDNA was inserted into the NotI site of pcDNA3 (5.4 kb; Invitrogen, Life Technologies Japan Ltd.), and a bovine growth hormone polyadenylation (BGHPA) sequence was inserted into the tail of the transgene to stabilize the expression. The entire nucleic acid sequence, containing a 0.6-kb cytomegalovirus (CMV) enhancer/promoter, the 0.8-kb hPRDX4 cDNA, and the 0.2-kb BGHPA sequence, was purified by restriction enzyme digestion with BglII and SmaI, and was microinjected into the male pronuclei of one-cell C57BL/6 mouse embryos using standard transgenic techniques to generate transgenic mice.

2. Provide better characterization of the wound healing process in mutant and WT mice (quantifications of the length and areas of the hyperproliferative epithelium at different time points after wounding, number of proliferating cells, etc.).

Response:

Thank you very much for your valuable suggestions. We presented Figure 1a and Supplementary Figure S1b with photographs of the wound healing process at various points in time (specifically, wounds 1, 3, 5, and 7 days after wound creation). In addition, the wound healing process in Figure 1b and Supplementary Figure S1b was changed from the diameter to the wound area (%), which was determined using the ImageJ software program. The modified figure is shown below.

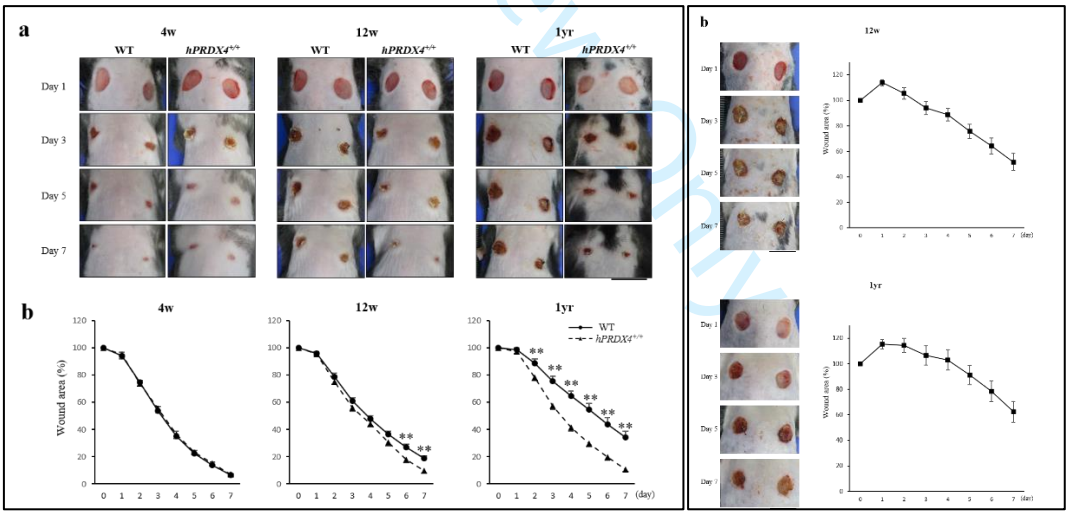

Furthermore, we performed histopathological and immunohistochemical analyses, which confirmed that there was no significant difference between WT and *hPRDX4* $^{+/+}$ in the length of the re-epithelialized epidermis or in the Ki-67 positive epithelial cells of the newly formed epidermis in each of the age group. The results are shown below and have been added to Supplementary Figure S5.

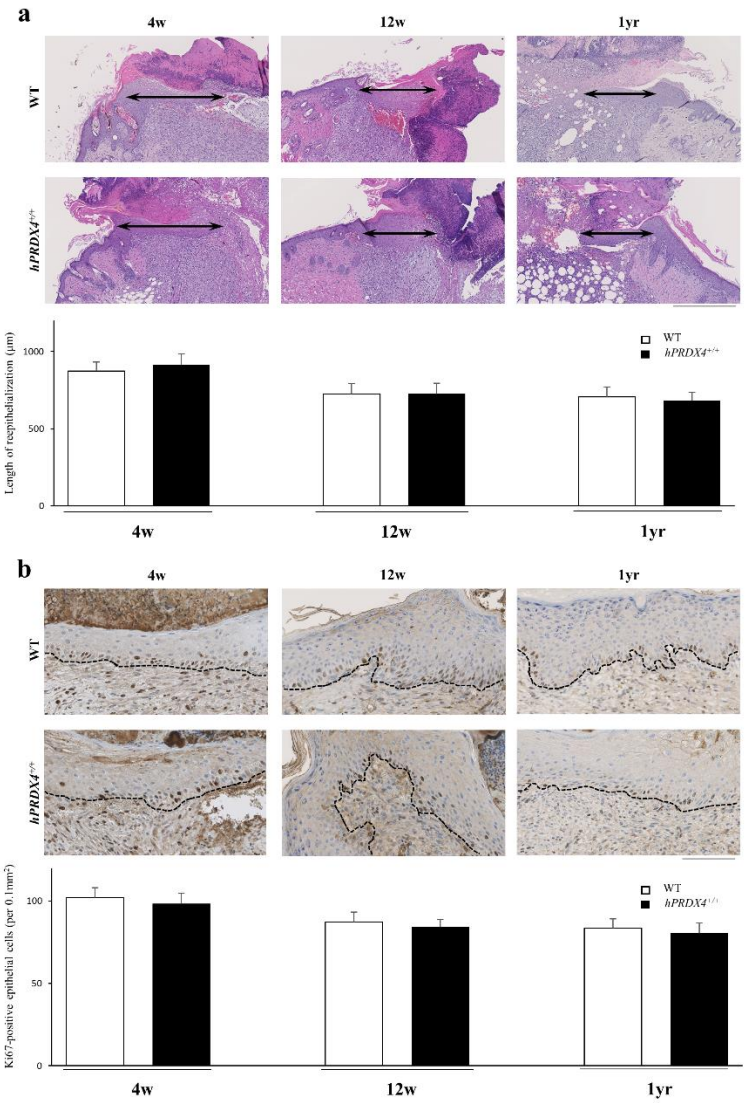

3. The authors need to consider the effects of hair follicle cycling on the wound healing process. Please, indicate in the manuscript that the dynamics of wound healing was assessed in the skin areas with all hair follicles at the same stage of the hair cycle (Anagen? Telogen?)

Response:

Thank you for your important suggestions. The hair cycle is composed of anagen, catagen and telogen phases, differences among these phases lead to changes in skin conditions, including dermal thickness, as well as various growth factors and cytokines[1)]. Therefore, skin wound healing experiments require a unified hair cycle, as the reviewer said.

The skin color of the C57BL/6 background mice that used in this study has been known to be pink for telogen and black to gray for anagen and catagen[1)] (Figure). In this study, we only used telogen-phase mice (pink skin). These were used in all *in vivo* and *in vitro* experiments. None of the mice were in the anagen or catagen (gray or black skin) phase. We mentioned the hair cycle of the mice in the 'Animals' section in 'SUPPLEMENTARY MATERIALS AND METHODS', as follows:

In order to avoid the effects of different phases of the hair cycle on wound healing, we only used telogen-phase mice for the *in vivo* and *in vitro* experiments.

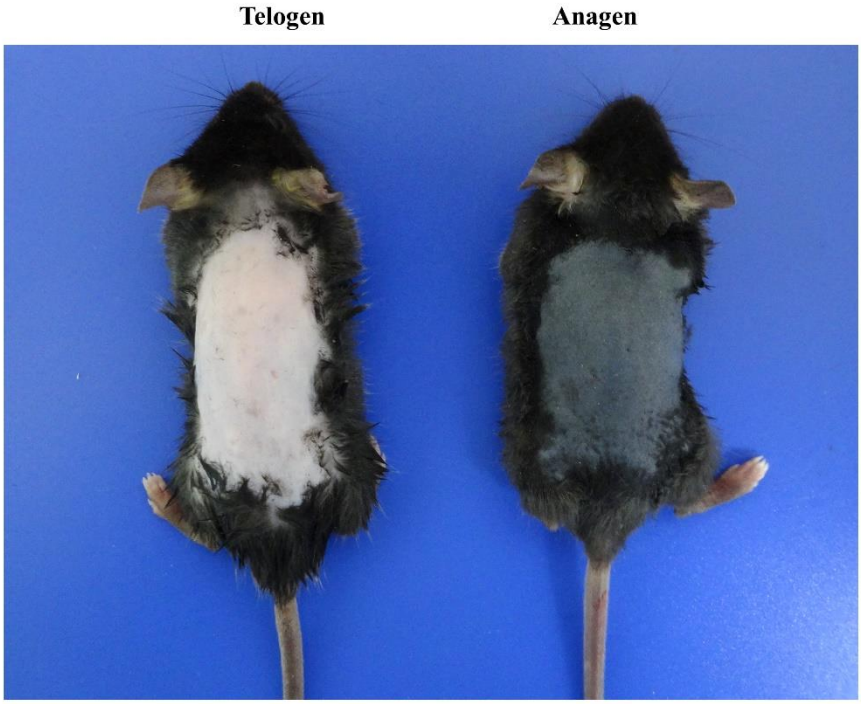

Ref. 1) Müller-Röver S, Handjiski B, van der Veen C, Eichmüller S, Foitzik K, McKay IA, et al. A comprehensive guide for the accurate classification of murine hair follicles in distinct hair cycle stages. J Invest Dermatol. 2001:117;3-15.

4. Discussion needs to be shortened by 20-30%.

The discussion of this paper may have been too long, which might have made it difficult to follow. We rewrote the Discussion and shortened it by approximately 25%. The revised manuscript should be more concise and clearer for readers.

Original Article

Peroxiredoxin 4 improved aging-related delayed wound healing in mice

Reimon Yamaguchi[1, 2], Xin Guo[1], Jianbo Zheng[1], Jing Zhang[1], Jia Han[1], Akihiro Shioya[1], Hidetaka Uramoto[3], Takashi Mochizuki[2], Sohsuke Yamada[1]

Department of [1]Pathology and Laboratory Medicine, [2]Dermatology and [3]Thoracic Surgery, Kanazawa Medical University, 1-1 daigaku, Uchinada, Ishikawa, 920-0293, Japan

ORCIDs

Reimon Yamaguchi: http://orcid.org/0000-0001-7084-1567

Xin Guo: http://orcid.org/0000-0002-5072-7000

Jianbo Zheng: http://orcid.org/0000-0002-0359-0451

Jing Zhang: http://orcid.org/0000-0002-9900-5009

Jia Han: http://orcid.org/0000-0003-0108-996X

Akihiro Shioya: http://orcid.org/0000-0002-1863-5368

Hidetaka Uramoto: http://orcid.org/0000-0003-4451-4225

Takashi Mochizuki: http://orcid.org/0000-0002-3793-980X

Sohsuke Yamada: http://orcid.org/0000-0003-2662-0024

Short title: PRDX4 in wound healing

***** Corresponding author: Xin Guo, M.D., Ph.D., Department of Pathology and Laboratory Medicine, Kanazawa Medical University, 1-1 Daigaku, Uchinada, Kahoku, Ishikawa, 920-0293, Japan. Tel: 81-76-2188021; Fax: 81-76-286-1207; and E-mail: tianqi11211216@yahoo.co.jp.

Key words: PRDX4, wound healing, oxidative stress, granulation tissue, fibroblast

Abbreviations:

PRDX, peroxiredoxin; WT, wild-type; *hPRDX4*$^{+/+}$, human *PRDX4*-transgenic; *PRDX4*$^{-/y}$, *PRDX4*-knockout ; IL-1β, interleukin 1 beta; FGF2, fibroblast growth factor 2; TGF-β1, transforming growth factor β1; PDGF, platelet derived growth factor; ROS, Reactive oxygen species; NF-κB , nuclear factor-kappa B; H&E, hematoxylin and eosin; α-SMA,

α-smooth muscle actin; TBARS, thiobarbituric acid reactive substance; 8-OHdG, 8-hydroxy-2'-deoxyguanosine; IHC, immunohistochemistry; H_2O_2, hydrogen peroxide; SOD1, Superoxide dismutase 1

Abstract

Aging-related delayed wound healing is an issue of concern worldwide. Oxidative stress is involved in wound healing. Antioxidative enzymes have various roles in this process. Peroxiredoxin 4 (PRDX4), a member of the PRDX family, is upregulated after injury. To investigate the effects of PRDX4 on aging-related wound healing, we subjected C57BL/6J (wild-type [WT]), human *PRDX4*-transgenic (*hPRDX4*$^{+/+}$), *PRDX4*-knockout (*PRDX4*$^{-/y}$) mice of three age groups (young, adult and aged) to skin wound formation. The overexpression of PRDX4 accelerated wound healing in adult and aged mice, but not young mice. Aged *hPRDX4*$^{+/+}$ mice showed reduced oxidative stress and inflammation, lower numbers of neutrophils, increased macrophage infiltration, increased angiogenesis, and increased growth factor levels. The granulation tissue of adult and aged *hPRDX4*$^{+/+}$ mice was richer in fibroblasts in comparison to matched WT mice. PRDX4 deficiency was associated with mortality in adult and aged mice. *In vitro*, the overexpression of PRDX4 promoted the proliferation and migration of fibroblasts derived from adult or aged mice and made fibroblasts more resistant to the cytotoxicity of hydrogen peroxide. PRDX4 is essential for wound healing and can improve the healing process from multiple aspects, suggesting that it may be very beneficial to wound treatment, especially for the elderly.

Introduction

With the progress of clinical medicine, the elderly population is gradually increasing, and society is aging (Kanasi et al., 2016). More and more attention has been paid to the care of the elderly. Due to limitations in mobility, aged people, especially those who stay in bed for long periods of time, are more susceptible to skin injury caused by pressure and shear force (Pittman, 2007). Aging is becoming an increasingly important aspect in the study of wound healing. In comparison to young people, skin wounds in the elderly show significantly delayed healing, which is associated with serious complications, mortality and high treatment costs (Keylock et al., 2008, Hardman et al., 2008). It is therefore of great significance to understand the causes and mechanisms of delayed wound healing in the elderly and to identify suitable treatments.

Wound healing is an intricate biological process that consists of three overlapping but distinct phases: the inflammatory, proliferative and remodeling phases. In the inflammatory phase, large numbers of inflammatory cells are recruited under the guidance of chemokines to fight infection and cleanse the wound (Rodrigues et al., 2019). Various cytokines are released by these cells, some of which (e.g., interleukin 1 beta [IL-1β] and tumor necrosis factor α [TNFα]), can affect the progression of the inflammatory phase (Eming et al., 2014). The proliferative phase is characterized by the replacement of

blood clot with fleshy granulation tissue formed by activated fibroblasts (Sgonc and Gruber, 2013). From the beginning of the proliferative phase, activated fibroblasts migrate into the wound bed and proliferate in response to growth factors, such as fibroblast growth factor 2 (FGF2), transforming growth factor β1 (TGF-β1) and platelet derived growth factor (PDGF), serving as a scaffold for other cells and components (Sgonc et al., 2013, Bainbridge, 2013). In addition to fibroblasts, macrophages are another important element in granulation tissue and a key player during the inflammatory to proliferative phase (Kim and Mair, 2019). The absence of macrophages in this period will reduce granulation tissue formation, resulting in delayed wound healing, whereas the local injection of macrophages can promote wound repair (Sorg et al., 2017, Danon D et al., 1989).

Reactive oxygen species (ROS) are generated during normal metabolic processes and take part in various physiological cell signaling processes, which are enhanced and centrally involved in the whole process of wound healing (Sen and Roy, 2008). Low concentrations of ROS are required to kill microorganism and stimulate cell survival signaling; however, the excessive accumulation causes oxidative stress and impaired wound healing (Dunnill et al., 2017, Bryan et al., 2012). The production of ROS is dramatically elevated in aging individuals, leading to severe extracellular and

intracellular oxidative stress, which damages the surrounding tissue and suppresses cell vitality, delaying wound healing (Cano Sanchez et al., 2018, Kurahashi et al., 2015). Antioxidative enzymes exist abundantly and regulate redox homeostasis in the skin; many have been proven to be involved in wound healing (Kurahashi et al., 2015). Peroxiredoxin 4 (PRDX4), an enzyme catalyzing the detoxification of hydrogen peroxide, is a unique secreted member of the PRDX family (Yamada and Guo, 2018). In a series of previous studies, we reported that PRDX4 had important anti-oxidative anti-inflammatory roles and was important for the regulation of cell vitality, including proliferation and migration in chronic inflammatory diseases and cancer (Guo et al., 2012, Nabeshima et al., 2013, Guo et al., 2019, Zheng et al., 2020). A study showed that the mRNA expression of PRDX4 was increased at day 5-8 after injury, implying that it may be involved in the wound healing process (Kümin et al., 2007). However, the precise roles and the mechanism through which this enzyme is involved in wound healing remain unknown.

In this study, we subjected C57BL/6J (wild-type [WT]), human PRDX4-transgenic (*hPRDX4*$^{+/+}$), *PRDX4*-knockout (*PRDX4*$^{-/y}$) mice of three age groups (young, adult and aged) to skin wound formation, to investigate the effect of PRDX4 on aging-related wound healing. By harvesting fibroblasts from the normal skin of WT and *hPRDX4*$^{+/+}$ mice of these three age groups, we observed the effect of the overexpression

PRDX4 on the proliferation and migration of these cells, and on cell vitality under high oxidative stress *in vitro*. This study will give new insights that will improve the understanding of the control of proliferation, migration, and survival of fibroblasts, and will hopefully lead to new therapeutic strategies to improve wound healing, especially in elderly individuals.

Results

PRDX4 had crucial roles in the wound healing of adult and aged mice.

In line with the results of an mRNA analysis (Kümin et al., 2007), the protein expression of PRDX4 in wound skin tissue was higher than that in normal skin tissue (Supplementary Figure 1a). After injury, the diameters of wounds on day 6–7 in adult *hPRDX4*$^{+/+}$ mice, and on day 2–7 in aged *hPRDX4*$^{+/+}$ mice, were significantly shorter in comparison to matched WT mice. However, in the young group, the diameters of wounds did not differ between the WT and *hPRDX4*$^{+/+}$ mice (Figure 1a, 1b). At 7 days after injury, hematoxylin and eosin (H&E) staining showed granulation tissues that were rich in cells and blood vessels in all young mice and in adult and aged *hPRDX4*$^{+/+}$ mice. In contrast, fewer cellular and vascular components were observed in the granulation tissues of adult and aged WT mice (Figure 1c). Moreover, severely impaired wound healing and high wound-related mortality were observed in the adult and aged *PRDX4*$^{-/y}$-knockout mice (Supplementary Figure S1b and Supplementary Table S1). **The three groups of mice showed no significant cutaneous phenotypic changes in histopathology or dermal thickness (Supplementary Figure S2a, S2b).** Thus, PRDX4 may be a key molecule in wound healing.

PRDX4 overexpression improved oxidative stress during wound healing

The immunohistochemistry (IHC), Western blotting and ELISA results showed the high expression of hPRDX4 in wound skin tissue and serum in all *hPRDX4*$^{+/+}$ mice (Figure 2a-c). With aging, the ratio of 8-hydroxy-2'-deoxyguanosine (8-OHdG)-positive cells in granulation tissue in WT mice was increased at 7 days after injury, and in adult and aged *hPRDX4*$^{+/+}$ mice this ratio was reduced in comparison to matched WT mice (Figure 2d). Moreover, at 7 days after injury, the thiobarbituric acid reactive substance (TBARS) levels in the serum of adult and aged *hPRDX4*$^{+/+}$ mice were significantly lower in comparison to matched WT mice (Figure 2e). Furthermore, in aged *hPRDX4*$^{+/+}$ mice, a lower level of H_2O_2 was observed (Figure 2f). The overexpression of PRDX4 could improve the severe local and systemic oxidative stress induced by wounds and aging.

PRDX4 overexpression suppressed the inflammatory response in the adult and aged groups.

The numbers of Gr-1-positive neutrophils in adult and aged *hPRDX4*$^{+/+}$ mice were significantly lower in comparison to matched WT mice, while the numbers of Mac-2-positive macrophages in aged *hPRDX4*$^{+/+}$ mice were significantly higher in comparison to aged WT mice (Figure 3a, 3b). The numbers of CD3-positive T cells did not differ between the WT and *hPRDX4*$^{+/+}$ mice in each age group (Supplementary Figure **S3**).

Similarly, the numbers of CD31-positive microvessels in adult and aged *hPRDX4*$^{+/+}$ mice were significantly increased in comparison to matched WT mice. (Figure 3c). In line with these results, the IL-1β, TNFα and nuclear factor-kappa B (NF-κB) expression levels in aged *hPRDX4*$^{+/+}$ mice were significantly reduced in comparison to aged WT mice (Figure 3d). These data indicated that the local inflammatory response after skin wound was enhanced and prolonged with aging, and that the overexpression of PRDX4 can suppress neutrophil infiltration and proinflammatory cytokines production, improving the prolonged inflammation phase induced by aging.

PRDX4 overexpression promoted granulation tissue formation in adult and aged mice.

In the adult and aged groups, the granulation area with α-smooth muscle actin (α-SMA)-positive cells was significantly larger in *hPRDX4*$^{+/+}$ mice than in WT mice (Figure 4a); similar results were observed regarding the number of α-SMA-positive myofibroblasts per defined area (Figure 4b). IHC showed that the number of ki-67-positive cells in granulation tissue decreased with aging in WT mice, and more ki-67-positive cells were found in adult and aged *hPRDX4*$^{+/+}$ mice, in comparison to matched WT mice (Figure 4c), revealing that the proliferative capacity in adult and aged mice was higher in

comparison to matched WT mice. Western blotting showed that the cyclin D1 and vimentin expressions levels were consistent with the results of ki-67 staining (Figure 4d). Moreover, the FGF2 levels in wound skin tissue and serum of aged *hPRDX4*$^{+/+}$ mice were higher than those in aged WT mice; however, no difference was found in the adult group (Figure 4e, 4f). The TGF-β1 and PDGF-BB levels did not differ between WT and *hPRDX4*$^{+/+}$ mice in each age group (Supplementary Figure **S4**). Next, we examined the expression of downstream genes related to the FGF2 pathway in the aged group. Western blotting showed that the ERK signaling pathways, which involve ERK1/2, p-cJUN and p-cFOS, were highly activated in aged *hPRDX4*$^{+/+}$ mice (Figure 4g). **Furthermore, there was no significant difference between WT and *hPRDX4*$^{+/+}$ in the length of the re-epithelialized epidermis and in the Ki-67-positive epithelial cells of the newly formed epidermis in each of the age group (Supplementary Figure S5). In addition, the collagen expression levels did not differ among the three groups (Supplementary Figure S6).** These results suggest that PRDX4 may promote granulation formation**, especially via fibroblast proliferation and migration,** by activating the FGF2/ERK signaling pathway in aged mice.

***In vitro*, PRDX4 overexpression reduced oxidative stress and promoted the proliferation and migration of skin fibroblasts.**

The high expression of hPRDX4 was confirmed in fibroblasts derived from the normal skin tissue of all *hPRDX4*$^{+/+}$ mice (Figure 5a, 5b). The intracellular TBARS and hydrogen peroxide H_2O_2 levels in fibroblasts increased with aging, and were lower in adult and aged *hPRDX4*$^{+/+}$ mice in comparison to matched WT mice (Figure 5c, 5d). In contrast, proliferative activity was decreased with aging, and significantly higher proliferative activity was observed in adult and aged *hPRDX4*$^{+/+}$ fibroblasts in comparison to matched WT fibroblasts (Figure 5e). The migration ability of these fibroblasts also decreased with aging, but the migration ability in all groups of *hPRDX4*$^{+/+}$ fibroblasts was significantly higher in comparison to matched WT fibroblasts (Figure 5f). These findings were supported by Western blotting to detect cyclin D1 and vimentin (Figure 5g).

Fibroblasts derived from *hPRDX4*$^{+/+}$ skin were more resistant to the cytotoxicity of H_2O_2.

To identify the protective effects of PRDX4 on cell viability, skin fibroblasts derived from young mice were exposed to H_2O_2 of different concentrations. With the increase in the H_2O_2 concentration, cell vitality was gradually inhibited in fibroblasts derived from WT

skin, however, under the same H_2O_2 condition, higher vitality was observed in fibroblasts derived from *hPRDX4*$^{+/+}$ skin (Figure 6a), suggesting that the inhibition of cell vitality was slowing down in these fibroblasts. Western blotting showed that the expression of cyclin D1 (Figure 6b) was consistent with the changes in cell vitality under different H_2O_2 concentrations. In contrast, the expression of cleaved caspase-3 increased with as the H_2O_2 concentration increased in fibroblasts derived from WT skin, and the lower expression of cleaved caspase-3 was found in fibroblasts derived from *hPRDX4*$^{+/+}$ skin (Figure 6b), indicating that the overexpression of PRDX4 protected fibroblasts from the cell apoptosis induced by high concentrations of H_2O_2. These results suggested that increased extracellular oxidative stress inhibited cell vitality and induced cell apoptosis, and that PRDX4, as a secretory protein, was effective for protecting cells from the damage caused by extracellular oxidative stress.

Discussion

In this study, the overexpression of PRDX4 accelerated wound healing in adult and aged mice, but no significant differences were observed in young mice. Similar results were also reported in Superoxide dismutase 1 (SOD1)-deficient and PRDX6-transgenic mice (Iuchi et al., 2010; Kümin et al., 2006). This seems to suggest that delayed wound healing may be improved by enhancing the expression of these antioxidative enzymes. However, unexpectedly, the overexpression of catalase, an enzyme catalyzing the dismutation of hydrogen peroxide, delayed wound healing in mice (Roy et al., 2006), suggesting that a certain level of ROS, especially H_2O_2, is crucial for promoting the healing process and that excessive antioxidant use may have adverse effects. Moreover, the protein expression of PRDX4 was increased in skin wound tissue, and its deficiency could lead to death in adult and aged wound mice. These observations imply that PRDX4 may play a crucial role in resisting lethal factors during wound healing.

After injury, neutrophils are first recruited to clean the wound. Neutrophil accumulation increases during the initial inflammatory phase and quickly declines from day 4 post-injury (Kim et al., 2008). At day 7 post-injury, numerous neutrophils are still present at the wound site in aged WT mice, and inflammatory

cytokines levels are higher in these mice than in young and adult mice. Studies show that early neutrophil infiltration increases with age due to an evident reduction in neutrophil activity in association with aging (Sgonc and Gruber, 2013), which explains why more neutrophils were found in aged WT mice. Neutrophil persistence and high proinflammatory cytokines levels will prolong the inflammatory phase and delay wound healing (Chen and Rogers, 2007, Barrientos et al., 2008). However, fewer neutrophils and reduced proinflammatory cytokines levels were observed in aged *hPRDX4*$^{+/+}$ mice in comparison to aged WT mice, suggesting that the prolonged inflammatory response was improved at the wound site, probably promoting healing in these mice. Furthermore, excessive neutrophil accumulation can lead to extracellular oxidant stress and neutrophil-generated ROS can directly trigger mitochondrial dysfunction (Zhang et al., 2018), damaging tissue and cells around the wound, and further amplifying the inflammatory response. The overexpression of PRDX4 in wound skin significantly improved the local and systemic oxidative stress status to protect wound tissue from oxidative damage, probably leading to reduced neutrophil infiltration in aged *hPRDX4*$^{+/+}$ mice.

Interestingly, in aged *hPRDX4*$^{+/+}$ mice, macrophage numbers were increased in comparison to the aged WT group. A large improvement of oxidative stress caused

by PRDX4 overexpression in aged mice may produce modified redox homeostasis, and alteration of ROS components may change capillary permeability (Sen and Roy, 2008) in skin wounds of these mice, facilitating monocyte infiltration. Moreover, aged mice showed delayed monocyte/macrophage infiltration in comparison to young mice (Sgonc and Gruber, 2013). The overexpression of PRDX4 may prevent the delay and allow monocytes to begin wound infiltration earlier, eventually leading to the accumulation of greater numbers of macrophages in the wound site in aged *hPRDX4*$^{+/+}$ mice. To avoid further damage in the wound, these macrophages will phagocytose infiltrated neutrophils and cell debris, which may also be an important contributor to the reduction in the number of neutrophils in the wounds of aged *hPRDX4*$^{+/+}$ mice.

FGF2 can accelerate granulation tissue formation by promoting fibroblast/myofibroblast proliferation and migration and angiogenesis (Behm et al., 2012). Delayed wound healing in aged mice is closely associated with the reduced expression of FGF2 (Swift et al., 1999). In this study, a reduced FGF2 level was observed in the wound skin tissue of aged WT mice, however, surprisingly, the level of this growth factor was dramatically increased in the wound skin tissue and serum of aged *hPRDX4*$^{+/+}$ mice, which may be a main reason for the improvement in the

delayed wound healing of these mice. It is unclear why FGF2 is elevated in the wound skin of aged *hPRDX4*$^{+/+}$ mice. Macrophages, a major cellular origin for FGF2, play important roles in granulation tissue formation and can promote wound healing by increasing FGF2 production (Takehara, 2000, Laplante et al., 2017). Thus, one possible explanation is that the massive aggregation of macrophages led to high local and systemic levels of FGF2 in aged *hPRDX4*$^{+/+}$ mice. Indeed, some key transcription factors related to the FGF2 signaling pathway, including Erk1/2, c-fos and c-Jun (Xiao et al., 2012, Cheng et al., 2007, Li et al., 2014), were activated in these mice. Thus, PRDX4 may promote granulation tissue formation through FGF2/Erk1/2 pathway activation, leading to the improvement of delayed wound healing.

However, this hypothesis is probably oversimplified, as although there were no significant differences in the expression of growth factors between the adult WT and *hPRDX4*$^{+/+}$ mice, higher cellular density and proliferation activity of myofibroblasts in granulation tissue were observed in adult *hPRDX4*$^{+/+}$ mice with a faster healing process. *In vitro*, the viability of fibroblasts derived from the normal skin of adult and aged *hPRDX4*$^{+/+}$ mice was significantly higher in comparison to the matched WT group. Normally, intracellular ROS can be maintained at a low level

by the regulatory role of the antioxidant system, and act as signaling molecules in cell proliferation, senescence and apoptosis (Cui et al., 2012). ROS production increases with age (Sohal et al., 1994), and high intracellular levels of ROS (e.g., H_2O_2) are closely associated with cell senescence, wherein cell proliferation is arrested (Lu and Finkel, 2008). Increased antioxidant levels delay this cellular process (Itahana et al., 2003, Serra et al., 2003). The overexpression of PRDX4 may properly reduce the intracellular ROS/H_2O_2 levels and delay senescence, leading to the enhanced proliferation of fibroblasts in adult and aged *hPRDX4*$^{+/+}$ mice. Thus, the promotion of fibroblast proliferation by the overexpression of PRDX4 may be an important reason for the accelerated wound healing observed in adult *hPRDX4*$^{+/+}$ mice.

Furthermore, with the increase in the H_2O_2 concentration in culture medium, cell vitality was obviously suppressed in WT fibroblasts; however, this suppression was improved in *hPRDX4*$^{+/+}$ fibroblasts (Figure 6a, 6b). Severe oxidative stress also induces cell apoptosis to suppress cell proliferation (Sinha et al., 2013). Thus, in aged *hPRDX4*$^{+/+}$ mice, PRDX4 overexpression not only promoted fibroblast proliferation but also inhibited the apoptosis of fibroblasts induced by high ROS/H_2O_2 levels.

Moreover, PRDX4 overexpression led to age-independent enhancement of

the migration capability of fibroblasts *in vitro*. The association between PRDX4 and cell migration was also reported in other studies, but in different types of cells it may regulate this cell behavior depending on different signaling (Wei et al., 2011; Zheng et al., 2020). The specific mechanism through which PRDX4 is involved in the regulation of fibroblast migration requires further investigation. However, during the wound healing process, in addition to the migration ability of cells themselves, various chemokines play important roles in fibroblast migration (Ridiandries et al., 2018). Thus, although the migration of skin fibroblasts was also significantly enhanced in young hPRDX4 mice, it did not affect the healing process in these mice.

In summary, the overexpression of PRDX4 significantly improved delayed wound healing by shortening the prolonged inflammatory phase, increasing growth factor production, and promoting fibroblast proliferation and migration in aged mice, while it only accelerated wound healing in the proliferative phase by upregulating fibroblast vitality in adult mice, suggesting that PRDX4 may be extremely beneficial to wound healing, especially in elderly individuals. Furthermore, in the young group, although faster wound healing was not found in *hPRDX4*$^{+/+}$ mice, the overexpression of PRDX4, at the very least, did not impair wound healing, implying that the application of this antioxidant enzyme in wound

treatment will not lead to worse outcomes in individuals with weaker oxidative stress.

Materials & Methods

Additional details are available online in the Supplementary Materials and Methods.

Mice

Male 4-week-old (young), 12-week-old (adult) and 1-year-old (aged) WT (C57BL/6), *hPRDX4*$^{+/+}$ and *PRDX4*$^{-/y}$ mice were used for the experiments. All experiments were conducted in accordance with the guidelines of the Ethics Committee of Animal Care and Experimentation, Kanazawa Medical University, Japan (protocol code: 2020-77).

Wound healing model

Following hair removal and disinfection and under anesthesia, a double 6-millimeter full-thickness wound was created at a dorsal site in all mice. **Wound sites were digitally photographed daily after wound creation, and the wound area was measured using the ImageJ software program (National Institutes of Health, Bethesda, MD, USA).** Mice were sacrificed at 7 days after injury and wound site skin tissue and serum were collected for experiments.

Primary fibroblast culture and treatment

A 1×1-cm piece of skin tissue was taken from the dorsum of mice in all groups. The skin tissue was then cut into 1-mm square small pieces, placed on a culture dish with DMEM containing 10% FBS and maintained in a humidified atmosphere at 37°C. The fibroblasts that migrated out of the skin were harvested and cultured. These fibroblasts were exposed to 2.5, 5, or 10 μM H_2O_2 respectively for 24 hours and then cell viability was measured.

Statistical analysis

Data were expressed as the mean ± standard error of the mean (SEM). An unpaired Student t test was performed to compare the values between two groups. *P* values of <0.05 were considered to indicate statistical significance.

Data Availability Statement

All relevant data for this article are contained within this manuscript, and any further inquiry can be made to the corresponding author.

ORCIDs

Reimon Yamaguchi: http://orcid.org/0000-0001-7084-1567

Xin Guo: http://orcid.org/0000-0002-5072-7000

Jianbo Zheng: http://orcid.org/0000-0002-0359-0451

Jing Zhang: http://orcid.org/0000-0002-9900-5009

Jia Han: http://orcid.org/0000-0003-0108-996X

Akihiro Shioya: http://orcid.org/0000-0002-1863-5368

Hidetaka Uramoto: http://orcid.org/0000-0003-4451-4225

Takashi Mochizuki: http://orcid.org/0000-0002-3793-980X

Sohsuke Yamada: http://orcid.org/0000-0003-2662-0024

Conflict of Interest

The authors declare no conflicts of interest in association with the present study.

Acknowledgements

This work was supported by Grant-in-Aid for Young Scientists (No: 20K17363 to Reimon Yamaguchi and No: 19K16783 to Xin Guo) and Grant-in-Aid for Scientific Research (No: 20K07454 to Sohsuke Yamada, 17K10803 to Hidetaka Uramoto) from the Ministry of Education, Culture, Sports, Science and Technology, Tokyo, Japan. We thank Yuka

Hiramatsu and Manabu Yamashita for their expert technical assistance.

Author Contributions

Conceptualization: R. Yamaguchi, X. Guo, S. Yamada

Data Curation: R. Yamaguchi, X. Guo, S. Yamada

Formal Analysis: R. Yamaguchi, X. Guo, S. Yamada

Funding Acquisition: R. Yamaguchi, X. Guo, H. Uramoto, S. Yamada

Investigation: R. Yamaguchi, X. Guo, J. Zheng, J. Zhang, J. Han,

A. Shioya, H. Uramoto, T. Mochizuki, S. Yamada

Methodology: R. Yamaguchi, X. Guo, J. Zheng, J. Zhang, J. Han, A. Shioya

Project Administration: R. Yamaguchi, X. Guo, S. Yamada

Resources: R. Yamaguchi, X. Guo, S. Yamada

Software: R. Yamaguchi, X. Guo, A. Shioya

Supervision: X. Guo, S. Yamada

Validation: R. Yamaguchi, X. Guo, S. Yamada

Visualization: R. Yamaguchi, X. Guo, S. Yamada

Writing - Original Draft Preparation: R. Yamaguchi, X. Guo

Writing - Review and Editing: R. Yamaguchi, X. Guo, S. Yamada

References

Bainbridge P. Wound healing and the role of fibroblasts. J Wound Care 2013;22:407-8, 410-12.

Barrientos S, Stojadinovic O, Golinko MS, Brem H, Tomic-Canic M. Growth factors and cytokines in wound healing. Wound Repair Regen. 2008;16:585–601.

Behm B, Babilas P, Landthaler M, Schreml S. Cytokines, chemokines and growth factors in wound healing. J Eur Acad Dermatol Venereol 2012;26:812–20.

Bryan N, Ahswin H, Smart N, Bayon Y, Wohlert S, Hunt JA. Reactive oxygen species (ROS)—A family of fate deciding molecules pivotal in constructive inflammation and wound healing. Eur Cells Mater 2012;24:249–65.

Cano Sanchez M, Lancel S, Boulanger E, Neviere R. Targeting Oxidative Stress and Mitochondrial Dysfunction in the Treatment of Impaired Wound Healing: A Systematic Review. Antioxidants (Basel) 2018;7:98.

Chen WY, Rogers AA. Recent insights into the causes of chronic leg ulceration in venous diseases and implications on other types of chronic wounds. Wound Repair Regen 2007;15:434–49.

Cheng B, Liu HW, Fu XB, Sun TZ, Sheng ZY. Recombinant human platelet-derived

growth factor enhanced dermal wound healing by a pathway involving ERK and c-fos in diabetic rats. J Dermatol Sci 2007;45:193-201.

Cui H, Kong Y, Zhang H. Oxidative stress, mitochondrial dysfunction, and aging. J Signal Transduct. 2012;2012:646354.

Danon D, Kowatch MA, Roth GS. Promotion of wound repair in old mice by local injection of macrophages. Proc Natl Acad Sci U S A 1989;86:2018-20.

Dunnill C, Patton T, Brennan J, Barrett J, Dryden M, Cooke J, et al. Reactive oxygen species (ROS) and wound healing: The functional role of ROS and emerging ROS-modulating technologies for augmentation of the healing process. Int Wound J 2017;14:89–96.

Eming SA, Martin P, Tomic-Canic M. Wound repair and regeneration: mechanisms, signaling, and translation. Sci Transl Med 2014;6:265sr6.

Guo X, Noguchi H, Ishii N, Homma T, Hamada T, Hiraki T, et al. The Association of Peroxiredoxin 4 with the Initiation and Progression of Hepatocellular Carcinoma. Antioxid Redox Signal 2019;30:1271-84.

Guo X, Yamada S, Tanimoto A, Ding Y, Wang KY, Shimajiri S, et al. Overexpression of peroxiredoxin 4 attenuates atherosclerosis in apolipoprotein E-knockout mice. Antioxid Redox Signal 2012;17:1362-75.

Hardman MJ, Ashcroft GS. Estrogen, not intrinsic aging, is the major regulator of delayed human wound healing in the elderly. Genome Biol 2008;9:R80.

Itahana K, Zou Y, Itahana Y, Martinez JL, Beausejour C, Jacobs JJL, et al. Control of the replicative life span of human fibroblasts by p16 and the polycomb protein Bmi-1. Mol Cell Biol 2003;23:389–401.

Iuchi Y, Roy D, Okada F, Kibe N, Tsunoda S, Suzuki S, et al. Spontaneous skin damage and delayed wound healing in SOD1-deficient mice. Mol Cell Biochem 2010;341:181–94.

Kanasi E, Ayilavarapu S, Jones J. The aging population: demographics and the biology of aging. Periodontol 2000 2016;72:13-8.

Keylock KT, Vieira VJ, Wallig MA, DiPietro LA, Schrementi M, Woods JA. Exercise accelerates cutaneous wound healing and decreases wound inflammation in aged mice. Am J Physiol Regul Integr Comp Physiol 2008;294:R179-84.

Kim MH, Liu W, Borjesson DL, Curry FRE, Miller LS, Cheung AL, et al. Dynamics of neutrophil infiltration during cutaneous wound healing and infection using fluorescence imagin. J Invest Dermatol 2008;128:1812–20.

Kim SY, Nair MG. Macrophages in wound healing: activation and plasticity. Immunol Cell Biol 2019;97:258-67.

Kümin A, Huber C, Rülicke T, Wolf E, Werner S. Peroxiredoxin 6 is a potent cytoprotective enzyme in the epidermis. Am J Pathol 2006;169:1194–205.

Kümin A, Schäfer M, Epp N, Bugnon P, Born-Berclaz C, Oxenius A, et al. Peroxiredoxin 6 is required for blood vessel integrity in wounded skin. J Cell Biol 2007;179:747–60.

Kurahashi T, Fujii J. Roles of Antioxidative Enzymes in Wound Healing. J Dev Biol 2015;3:57-70.

Laplante P, Brillant-Marquis F, Brissette MJ, Joannette-Pilon B, Cayrol R, Kokta V, et al. MFG-E8 Reprogramming of Macrophages Promotes Wound Healing by Increased bFGF Production and Fibroblast Functions. J Invest Dermatol 2017;137:2005–13.

Li T, Song T, Ni L, Yang G, Song X, Wu L, et al. The p-ERK-p-c-Jun-cyclinD1 pathway is involved in proliferation of smooth muscle cells after exposure to cigarette smoke extract. Biochem Biophys Res Commun 2014;453:316-20.

Lu T, Finkel T. Free radicals and senescence. Exp Cell Res 2008;314:1918–22.

Nabeshima A, Yamada S, Guo X, Tanimoto A, Wang KY, Shimajiri S, et al. Peroxiredoxin 4 protects against nonalcoholic steatohepatitis and type 2 diabetes in a nongenetic mouse model. Antioxid Redox Signal 2013;19:1983-98.

Pittman J. Effect of aging on wound healing: current concepts. J Wound Ostomy Continence Nurs 2007;34:412-5.

Ridiandries A, Tan JTM, Bursill CA. The Role of Chemokines in Wound Healing. Int J Mol Sci 2018;19:3217.

Rodrigues M, Kosaric N, Bonham CA, Gurtner GC. Wound Healing: A Cellular Perspective. Physiol Rev 2019;99:665-706.

Roy S, Khanna S, Nallu K, Hunt TK, Sen CK. Dermal wound healing is subject to redox control. Mol Ther 2006;13:211–20.

Sen CK, Roy S. Redox signals in wound healing. Biochim Biophys Acta 2008;1780:1348–61.

Serra V, Zglinicki TV, Lorenz M, and Saretzki G. Extracellular superoxide dismutase is a major antioxidant in human fibroblasts and slows telomere shortening. J Biol Chem 2003;278:6824–30.

Sgonc R, Gruber J. Age-related aspects of cutaneous wound healing: a mini-review. Gerontology 2013;59:159-64.

Sinha K, Das J, Pal PB, Sil PC. Oxidative stress: the mitochondria-dependent and mitochondria-independent pathways of apoptosis. Arch Toxicol 2013;87:1157–80.

Sohal RS, Dubey A. Mitochondrial oxidative damage, hydrogen peroxide release, and aging, Free Radic Biol Med 1994;16:621–6.

Sorg H, Tilkorn DJ, Hager S, Hauser J, Mirastschijski U. Skin Wound Healing: An Update

on the Current Knowledge and Concepts. Eur Surg Res 2017;58:81-94.

Swift ME, Kleinman HK, DiPietro LA. Impaired wound repair and delayed angiogenesis in aged mice. Lab Invest 1999;79:1479–87.

Takehara K. Growth regulation of skin fibroblasts. J Dermatol Sci 2000;24 Suppl 1:S70–7.

Wei Q, Jiang H, Xiao Z, Baker A, Young MR, Veenstra TD, et al. Sulfiredoxin-Peroxiredoxin IV axis promotes human lung cancer progression through modulation of specific phosphokinase signaling. Proc Natl Acad Sci U S A 2011;108:7004–9.

Xiao L, Du Y, Shen Y, He Y, Zhao H, Li Z. TGF-beta 1 induced fibroblast proliferation is mediated by the FGF-2/ERK pathway. Front Biosci (Landmark Ed) 2012 Jun;17:2667–74.

Yamada S, Guo X. Peroxiredoxin 4 (PRDX4): Its critical in vivo roles in animal models of metabolic syndrome ranging from atherosclerosis to nonalcoholic fatty liver disease. Pathol Int 2018;68:91-101.

Zhang J, Guo X, Hamada T, Yokoyama S, Nakamura Y, Zheng J, et al. Protective Effects of Peroxiredoxin 4 (PRDX4) on Cholestatic Liver Injury. Int J Mol Sci 2018;19:2509.

Zheng J, Guo X, Shioya A, Yoshioka T, Matsumoto K, Hiraki T, et al. Peroxiredoxin 4 promotes embryonal hepatoblastoma cell migration but induces fetal cell differentiation.

Am J Transl Res 2020;12:2726-37.

FIGURE REGENDS

Figure 1.

Adult and aged *hPRDX4*$^{+/+}$ mice but not young mice showed accelerated wound healing. (a) The skin wound healing process. Representative results of 1 day and 7 days after injury are shown. Scale bar: 10 mm (b) **Changes in wound area as the percentage of the initial wound area for 7 days after injury are shown.** All values represent the mean ± SEM. **, P < 0.01, versus WT mice. n=15–18 per group. (c) Midline sections of wound with H&E staining at 7 days after injury are shown. Scale bar in low power view: 1 mm. Scale bar in high power view: 100 μm. n=8–10 groups.

Figure 2.

The overexpression of hPRDX4 reduced oxidative stress in wound healing. (a) Immunostaining of PRDX4 at 7 days after injury. scale bar: 50 μm. (b) Western blotting to detect PRDX4 in wound skin at 7 days after injury. (c) The ELISA to detect PRDX4 in serum at 7 days after injury. All values represent the mean ± SEM. **, P < 0.01, versus WT mice. n=15–18 per group. (d) The immunohistochemical analysis to detect 8-OHdG at 7 days after injury. scale bar: 50 μm. All values represent the mean ± SEM. *, P < 0.05, **, P < 0.01, versus WT mice. n=8–10 per group. (e, f) TBARS levels (e) and

hydrogen peroxide levels (f) of serum at 7 days after injury. All values represent the mean ± SEM. *, P < 0.05, **, P < 0.01, versus WT mice. n=15–18 per group.

Figure 3.

The inflammatory response was suppressed and angiogenesis was promoted in adult and aged *hPRDX4*$^{+/+}$ mice. (a, b) The immunohistochemical analysis to detect Gr-1 (a), Mac-2 (b) and CD31 (c) at 7 days after injury. scale bar: 50 μm. All values represent the mean ±SEM. *, P < 0.05, **, P < 0.01, versus WT mice. n=8–10 per group. (d) Western blotting to detect IL-1β, TNFα and NF-κB in wound skin at 7 days after injury.

Figure 4.

Granulation tissue formation was promoted in aged *hPRDX4*$^{+/+}$-transgenic mice.

(a, b) The immunohistochemical analysis to detect α–SMA at 7 days after injury. (a) Wound area contained α–SMA-positive cells. scale bar: 1 mm. (b) The density of α–SMA-positive cells per HPF. scale bar: 50 μm. All values represent the mean ± SEM. *, P < 0.05, **, P < 0.01, versus WT mice. n=8–10 per group. (c) The immunohistochemical analysis to detect Ki-67 at 7 days after injury. Scale bar: 50 μm. All values represent the mean ± SE. *, P < 0.05, versus WT mice. n=8–10 per group. (d)

Western blotting to detect cyclin D1 and vimentin in wound skin at 7 days after injury in the young, adult and aged groups. (e) Western blotting to detect FGF2 in wound skin at 7 days after injury in the adult and aged groups. (f) The ELISA to detect FGF2 in serum at 7 days after injury in the adult and aged groups. All values represent the mean ± SEM. *, $P < 0.05$, versus WT mice. n=15–18 per group. (g) Western blotting to detect ERK1/2, phosphorylated (p-) ERK1/2, cJUN, p-cJUN, cFOS, p-cFOS in wound skin at 7 days after injury in the aged group.

Figure 5.

The overexpression of PRDX4 reduced oxidative stress and promoted the proliferation and migration of mouse-derived skin fibroblasts *in vitro*.

(a) Immunofluorescent staining for PRDX4 in skin fibroblasts derived from young, adult and aged mice. scale bar: 25 μ m. (b) Western blotting to detect PRDX4 in skin fibroblast derived from young, adult and aged group. (c, d) The TBARS levels (c) and H_2O_2 levels (d) of lysates of skin fibroblast derived from young, adult and aged mice. The values per 1×10^6 cells are shown for each. All values represent the mean ± SEM. *, $P < 0.05$, **, $P < 0.01$, versus WT mice. n=5 per group. (e) The Cell Counting Kit-8 proliferation assay for skin fibroblasts derived from each generation. The cell viability measured at 0, 24, 48,

and 72 hours after seeding is shown. All values represent the mean ± SEM. *, P < 0.05, **, P < 0.01, versus WT mice. n=5 per group. (f) The cell migration assay for skin fibroblasts derived from each generation. Migrated cells were counted at 6 hours after seeding. scale bar: 50 μm. All values represent the mean ± SEM. **, P < 0.01, versus WT mice. n=5 per group. (g) Western blotting to detect cyclin D1 and vimentin in skin fibroblasts derived from each generation.

Figure 6.

Skin fibroblasts derived from *hPRDX4*$^{+/+}$ mice were resistant to the oxidative stress of H_2O_2.

(a) Exposure of cells to oxidative stress using H_2O_2 of different concentrations. Cell viability was expressed as the percentage of normal control. All values represent the mean ± SEM. **, P < 0.01, versus WT mice. n=5 per group. (b) Western blotting to detect cyclin D1, caspase3 and cleaved caspase3 in cell lysate of fibroblasts exposed to H_2O_2 of different concentrations.

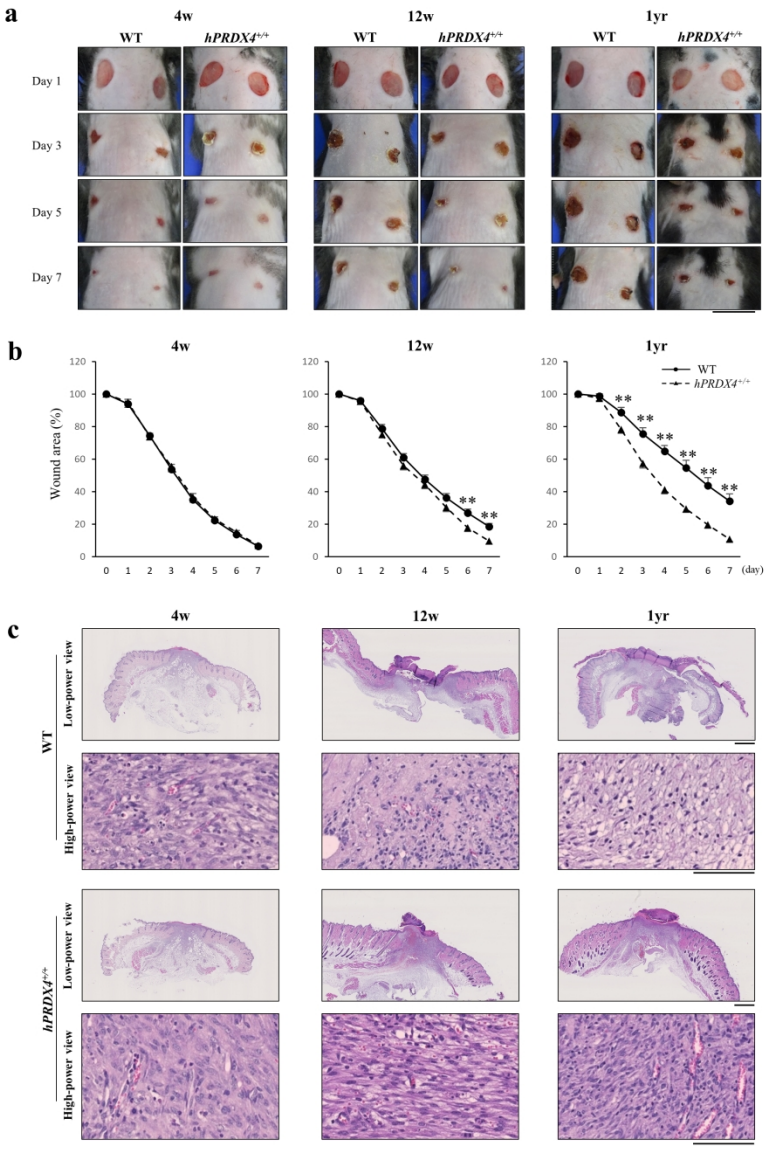

Figure1

190x275mm (300 x 300 DPI)

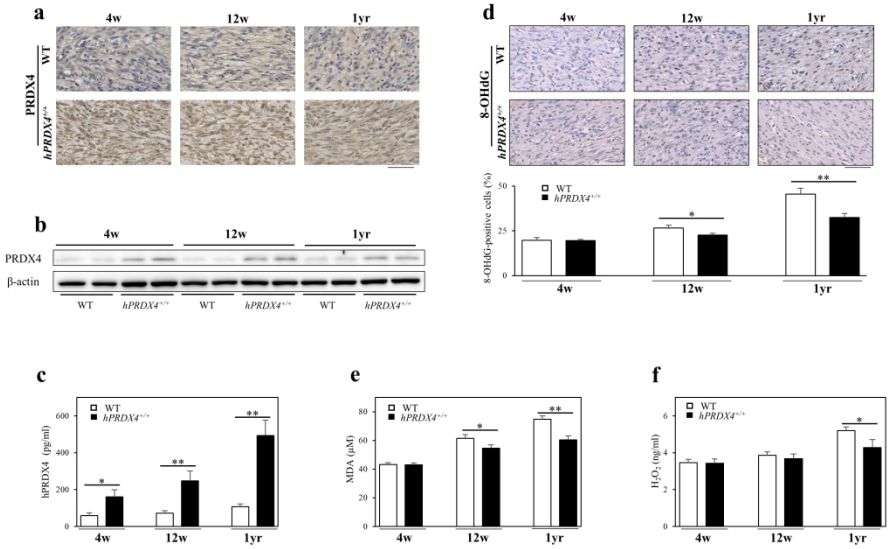

Figure2

275x190mm (300 x 300 DPI)

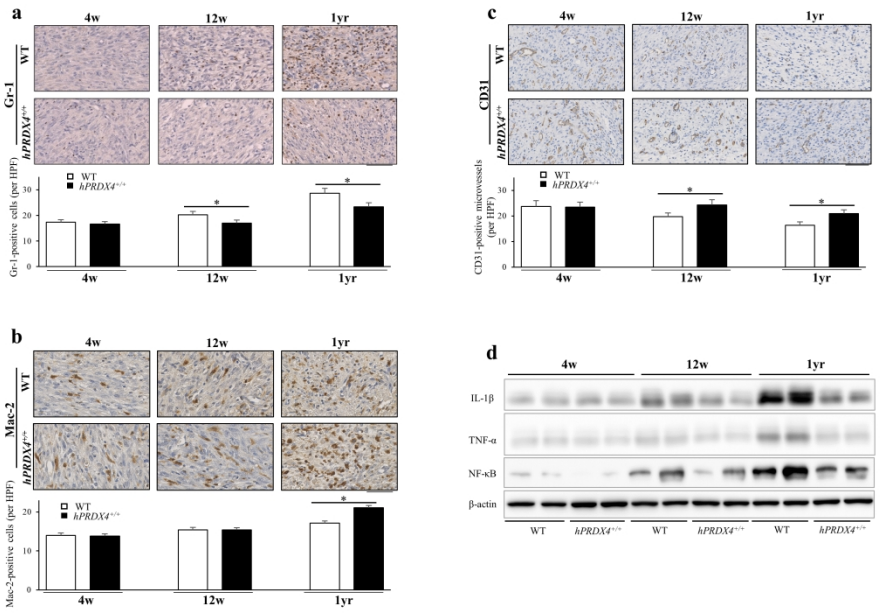

Figure3

275x190mm (300 x 300 DPI)

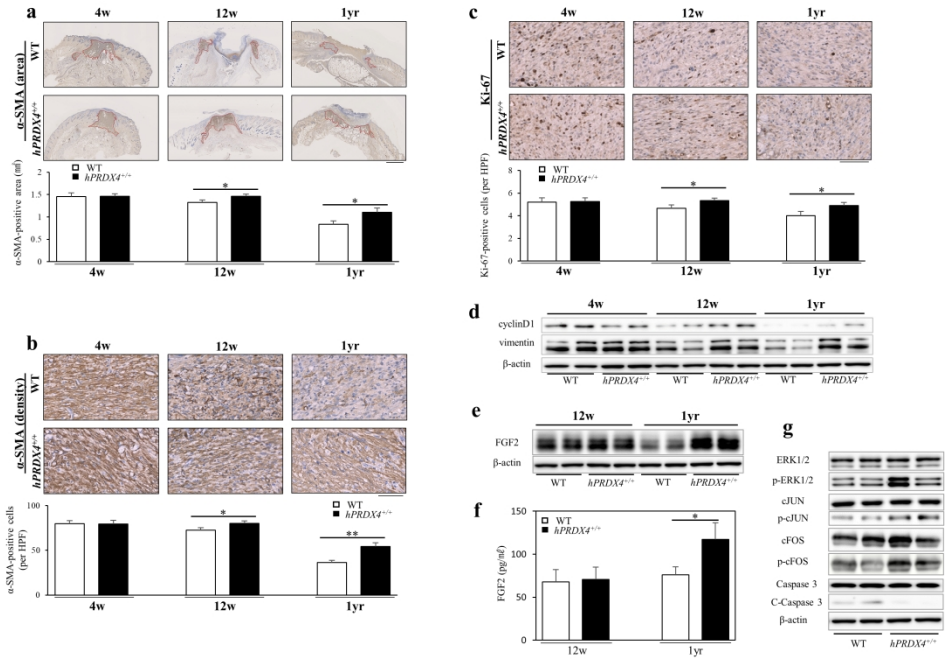

Figure4

275x190mm (300 x 300 DPI)

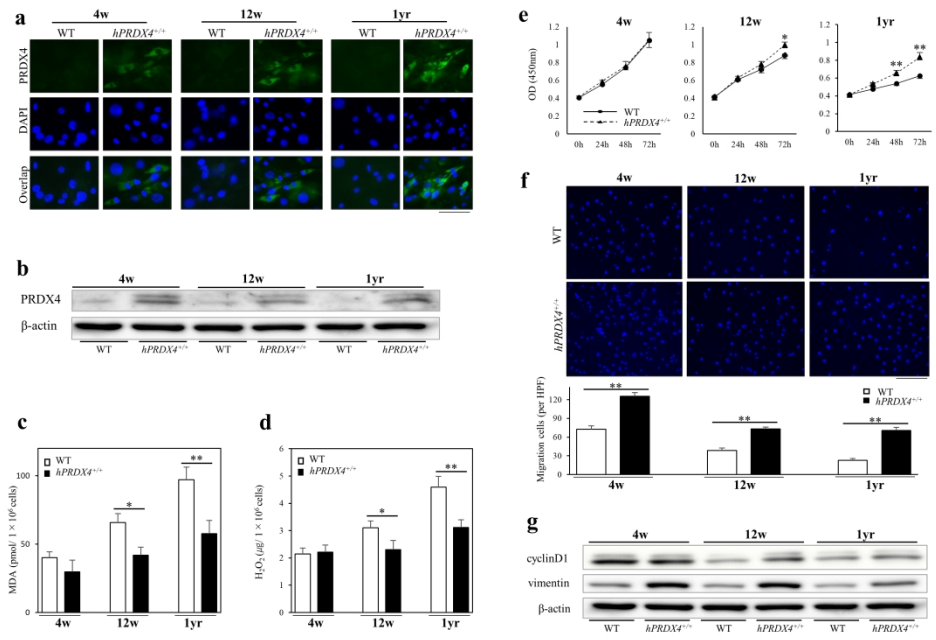

Figure5

275x190mm (300 x 300 DPI)

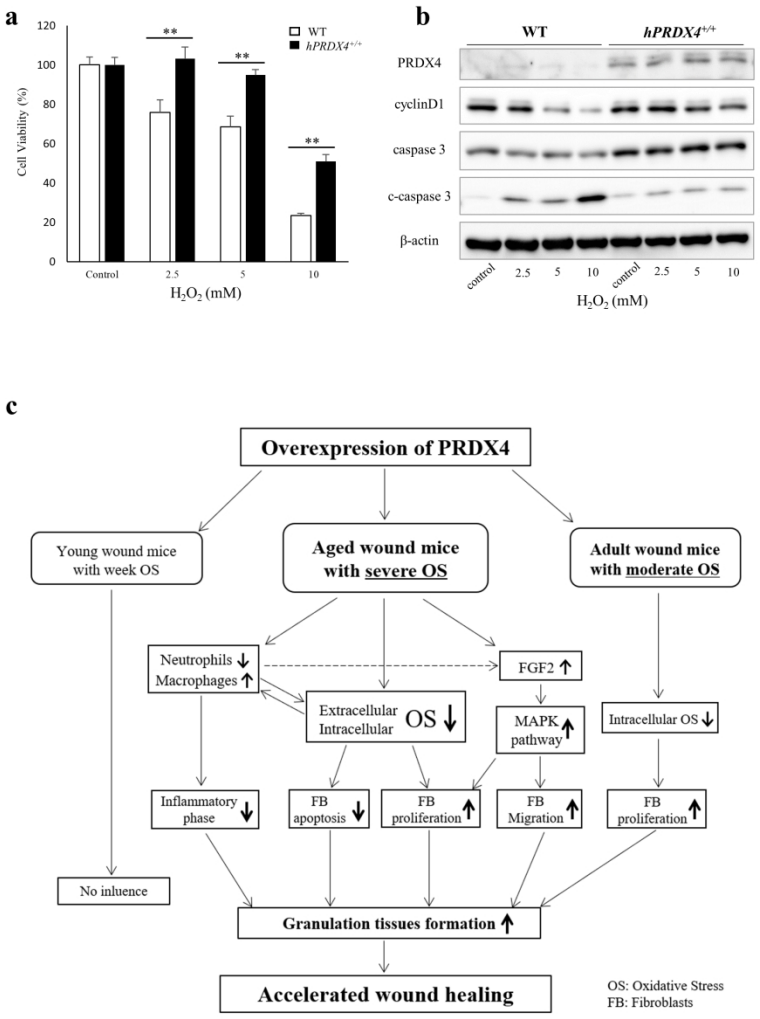

Figure6

190x275mm (300 x 300 DPI)

SUPPLEMENTARY RESULTS

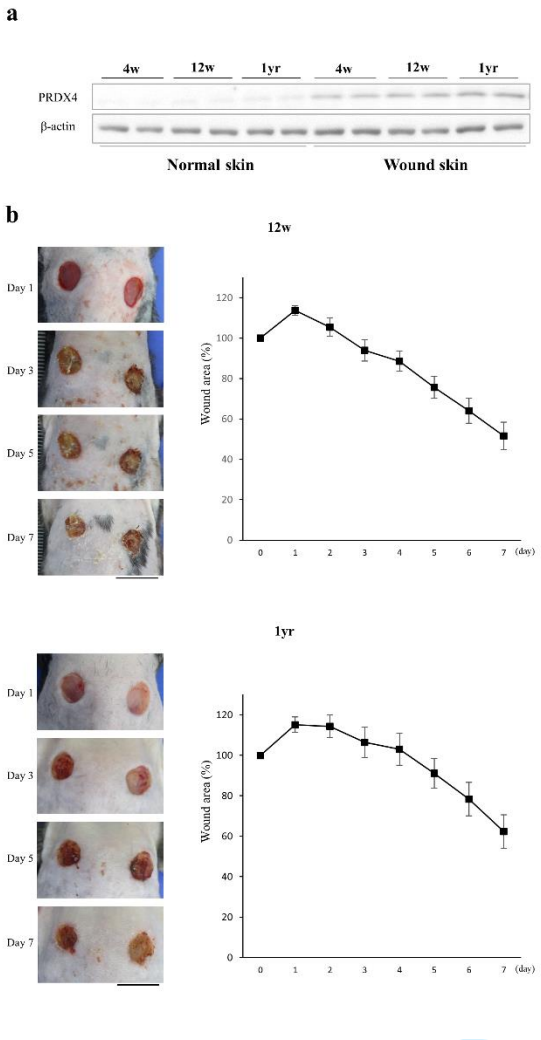

Supplementary Figure S1. PRDX4 is important for wound healing.

(a) Comparison of the PRDX4 expression in normal skin and wound skin by Western blotting in WT mice. (b) The skin wound healing process in *PRDX4*$^{-/y}$ mice. **Representative results at 7 days after wound creation are shown. Changes in the wound area are expressed as the percentage of the initial wound area.** Scale bar: 10 mm. All values represent the mean ± SE. n=8 per adult group, n=7 per aged group.

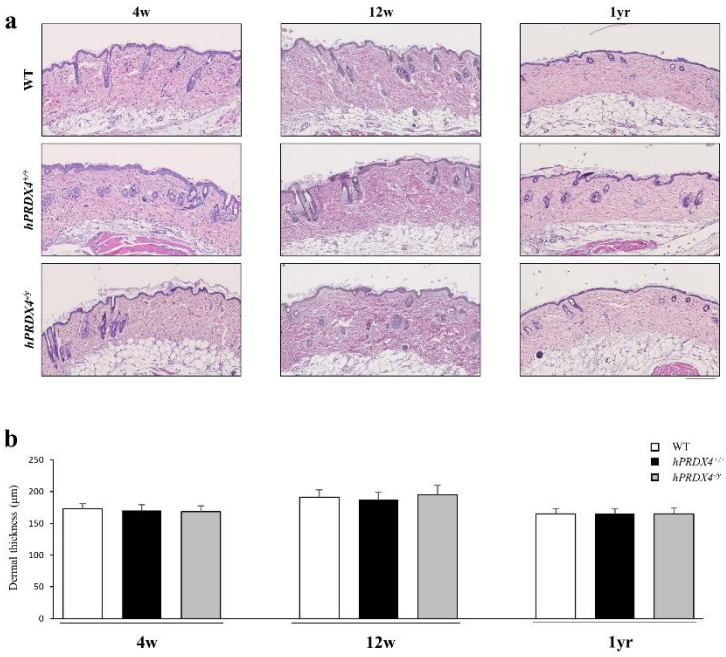

Supplementary Figure S2. Construction of the *hPRDX4*$^{+/+}$ mice, and comparison of skin phenotypic changes between wild-type (WT), *hPRDX4*$^{+/+}$ and *PRDX4*$^{-/y}$ mice.

(a) Representative histopathological images of normal dorsal skin in WT, *hPRDX4* $^{+/+}$ and *PRDX4* $^{-/y}$ mice are presented. scale bar: 100 μm. (b) Quantification of the dermal thickness of the dorsal skin in WT, *hPRDX4* $^{+/+}$ and *PRDX4* $^{-/y}$ mice. All values represent the mean ± SE. versus WT mice (n=5 per group).

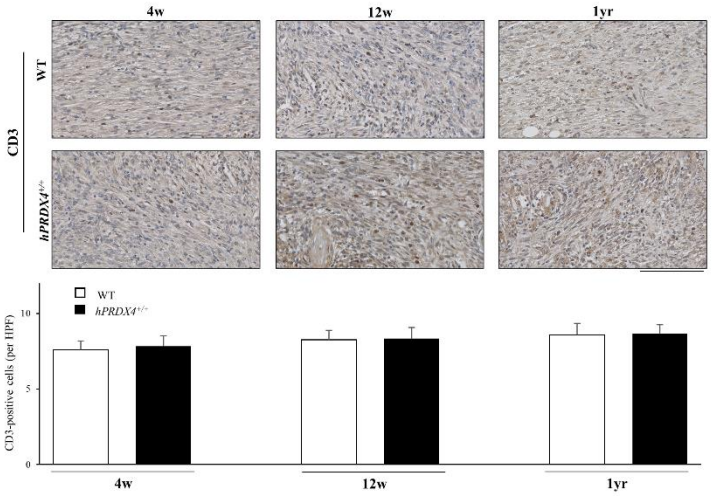

Supplementary Figure S3. The overexpression of PRDX4 had no effect in T lymphocyte infiltrate.

The immunohistochemical analysis to detect CD3 at 7 days after injury. scale bar: 50 μ m. All values represent the mean ± SE. versus WT mice. n=8–10 per group.

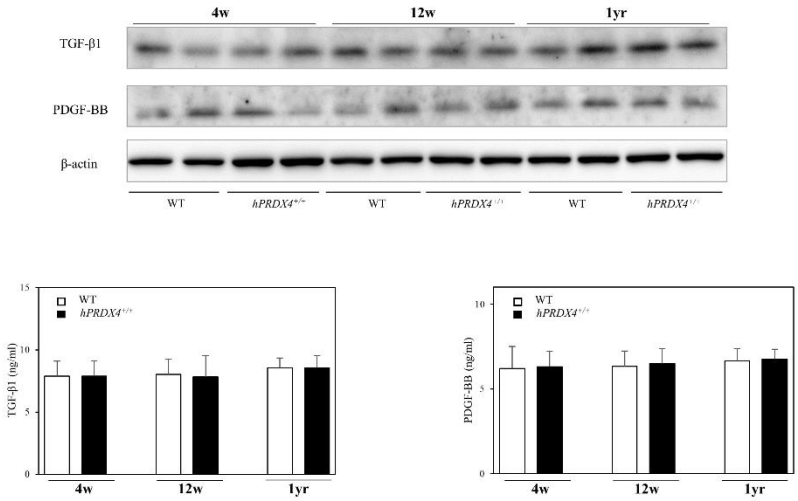

Supplementary Figure S4. The overexpression of PRDX4 did not affect the production of TGF-β1 and PDGF-BB.

(a) Western blotting to detect TGF-β1 and PDGF-BB in wound skin at 7 days after injury in the different age groups. (b, c) The ELISA to detect TGF-β1 (b) and PDGF-BB(c) in serum at 7 days after injury in the adult and aged groups. All values represent the mean ± SE. n=15–18 per group.

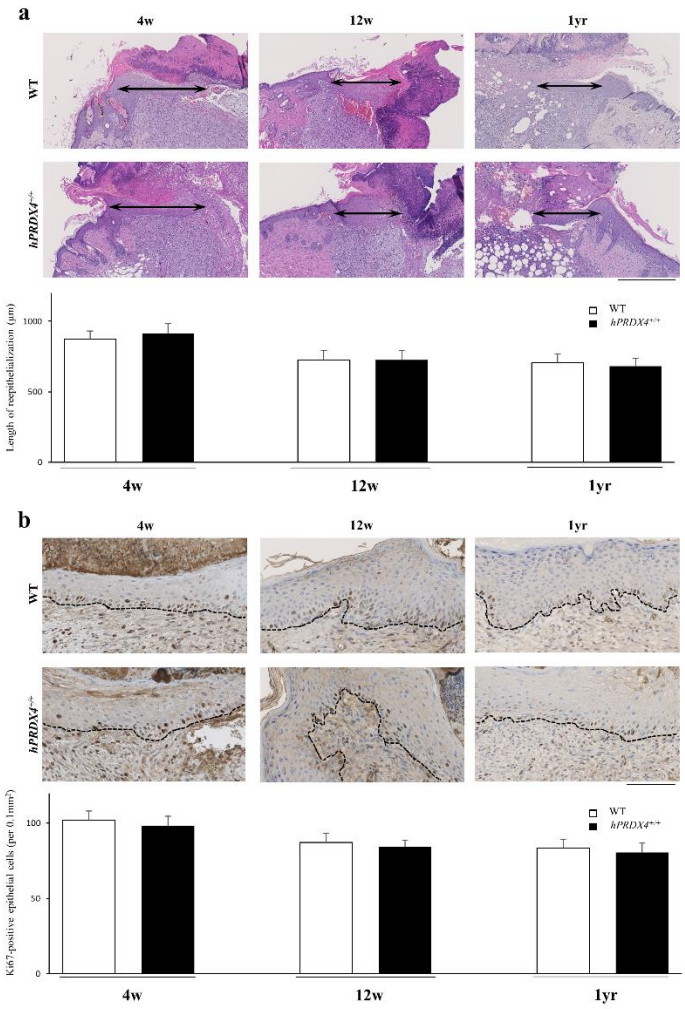

Supplementary Figure S5. The overexpression of hPRDX4 had no effect on re-epithelialization.

(a) A histopathological analysis of the length of re-epithelialized epidermis at 7 days after creation. Scale bar: 500 μm. All values represent the mean ± SE. n=8–10 groups. (b) The Ki-67 positive epithelial cells in newly formed epidermis. Dotted lines indicate the basement membrane. Scale bar: 100 μm. All values represent the mean ± SE. versus WT mice (n=8–10 per group).

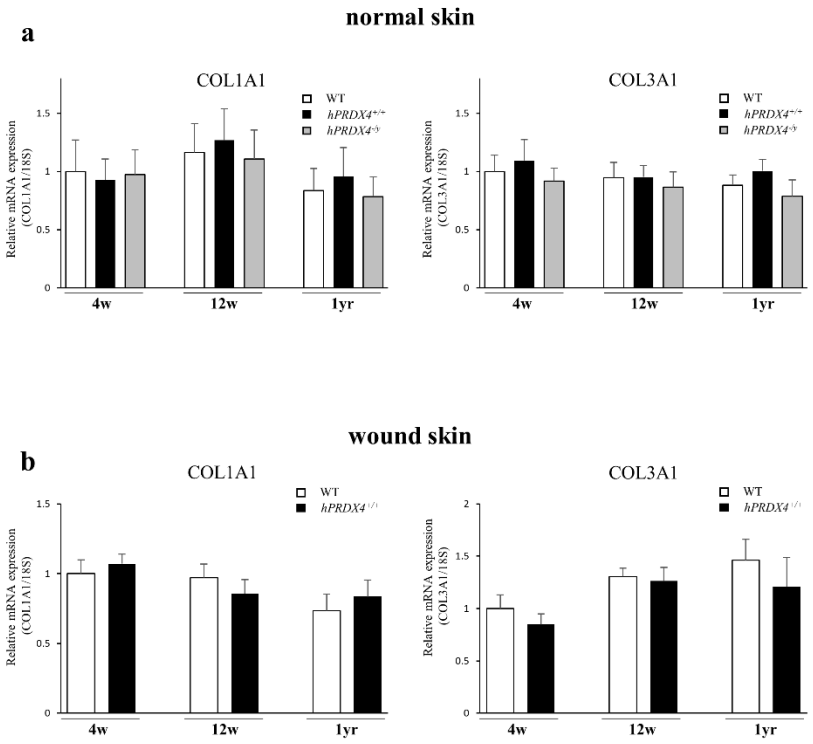

Supplementary Figure S6. The overexpression of hPRDX4 had no effect on the collagen expression of the skin.

(a) The expression of mRNA levels of type I and type III collagen in the dorsal normal skin in mice. The mRNA level in 4-week-old WT mice were assigned a value of 1. All values represent the mean ± SE (n=5 per group). (b) The mRNA expression levels of type

I and type III collagen in the wound skin in mice at 7 days after wounding. The mRNA level in 4-week-old WT mice were assigned a value of 1. All values represent the mean ± SE (n=5 per group).

hPRDX4$^{-/y}$	n	dead	Mortality rate (%)
12w	8	2	25.0
1yr	7	2	28.6

Supplementary Table S1. The mortality of PRDX4-knockout mice in the post-wound course.

SUPPLEMENTARY MATERIALS AND METHODS

Animals

Male C57BL/6 (WT) mice were purchased from Sankyo Labo Service Corporation, Inc., Japan. **The primers for hPRDX4 were designed based on a published sequence (Genebank accession no. NM_006406). hPRDX4 cDNA was amplified by reverse transcription–polymerase chain reaction and cloned into the pGEM-T easy vector system (Invitrogen, Life Technologies Japan Ltd., Tokyo, Japan) (Supplementary Figure S1a) (Guo et al., 2019, Guo et al., 2012, Yamada et al., 2012, Meier et al., 1996). The NotI fragment containing hPRDX4 cDNA was inserted into the NotI site of pcDNA3 (5.4 kb; Invitrogen, Life Technologies Japan Ltd.), and a bovine growth hormone polyadenylation (BGHPA) sequence was inserted into the tail of the transgene to stabilize the expression. The entire nucleic acid sequence, containing a 0.6-kb cytomegalovirus (CMV) enhancer/promoter, the 0.8-kb hPRDX4 cDNA, and the 0.2-kb BGHPA sequence, was purified by restriction enzyme digestion with BglII and SmaI, and was microinjected into the male pronuclei of one-cell C57BL/6 mouse embryos using standard transgenic techniques to generate transgenic mice. The *PRDX4* $^{-/y}$ mice were previously generated by Fujii et al (Iuchi et al., 2009) by cloning and sequencing mPRDX4 genomic DNA from a b129/SVJ mouse genomic library**

(Stratagene), and constructing a targeting vector using the cloned DNA fragment. As the chimeric male mice generated from the embryonic stem cells were infertile, they performed intracytosolic sperm injection into blastocysts and implanted them into the uteri of pseudopregnant C57BL/6 female mice. Mice were maintained and bred in a temperature- and light-controlled facility with *ad libitum* to water. Male WT, *hPRDX4*$^{+/+}$and *PRDX4*$^{-/y}$ (4 weeks old; 17–20 g, 12 weeks; 20-25g, 1 year old; 27-33g) mice were used for the experiments. **In order to avoid the effects of different phases of the hair cycle on wound healing, we only used telogen-phase mice for the *in vivo* and *in vitro* experiments.**

Wound healing model

All mice were anesthetized with a mixture of ketamine 50 mg/kg (Daiichi Sankyo Co., Tokyo, Japan) and medetomidine 1 mg/kg, (Meiji Yakuhin Co., Tokyo, Japan). The dorsal skin was then shaved and the remaining hair was removed with a depilatory cream. After cleaning with 70% ethanol, two six-millimeter full-thickness wounds per mouse were created at dorsal sites using a sterile disposable biopsy punch (Kai Industries, Gifu, Japan) under anesthesia. **Wound sites were digitally photographed daily after wound creation, and two average wound areas were measured on photographs using the**

Image J software program (version 1.53e, National Institutes of Health, Bethesda, MD, USA). Changes in the wound area are expressed as the percentage of initial wound area. At day 7 post-injury (n=15–18 per group), the mice were euthanized in a fed state by the intraperitoneal anesthetization of an overdose of ketamine (100 mg/kg) (Daiichi Sankyo Co.) and medetomidine (2 mg/kg) (Meiji Yakuhin Co.). The healing skin and normal skin surrounding wound were fixed in 10% neutral-buffered formalin and embedded in paraffin for a histologic examination. Frozen samples of the healing skin and normal skin were also stored for a protein assay.

The histopathological analysis and IHC of the wound site

Paraffin-embedded skin wound samples were sectioned at 4 μm and stained with hematoxylin and eosin (H＆E, Sigma). For immunohistochemical staining, the sections were incubated for 30 minutes with PBS containing 1% normal serum corresponding to the secondary antibodies and 1% BSA to inhibit nonspecific reactions. Antigen-retrieval was performed by heating slides to 95°C for 20 min in 0.01 M citrate buffer (pH 6.0) in a pressure cooker. The following primary antibodies and dilutions were used: PRDX4 (1:1000, Thermo Fisher Scientific), α-SMA (1:500, Dako Cytomation), 8-OHdG (1:200, Japan Institute for the Control of Aging), Gr-1 (1:500,), Mac-2 (1:1000, Cedarlane

Laboratories Ltd.), CD3 (1:1000, Abcam), Ki-67 (1:1000, Abcam), CD31(1:200, Dianova GmbH). The sections were incubated with the primary antibodies at 4°C overnight. After incubation with biotinylated secondary antibodies (Nichirei Bioscience Inc., Tokyo, Japan), immune complexes were visualized by the ABC peroxidase method (Nichirei Bioscience Inc.). **The length of the re-epithelialized epidermis was defined as the distance from the advancing tip of the re-epithelialization lip to the site of the first hair follicle at the wound margin, as previously reported (Chen et al., 2017, Shirakata et al., 2005).** The wound lesion was defined as the area surrounded by normal skin tissue and fascia, regenerated epidermis, and crust, and epithelium was excluded from the evaluation. In IHC, 8–10 samples per group were evaluated and averaged. The numbers of 8-OHdG-positive cells, Gr-1-positive neutrophils, F4/80+ macrophages, CD3+ T cells, CD31-positive microvessels, α-SMA-positive fibroblasts/myofibroblasts, and ki-67-positive cells in the wound lesion were measured on 5 randomly chosen in high power fields of sections per individual, and the average of the selected 5 fields was calculated. The wound area containing α-SMA-positive cells was measured using the freehand tool of the NanoZoomer Digital Pathology Virtual Slide Viewer software program (Hamamatsu Photonics Corp, Hamamatsu, Japan). All measurements were performed by two pathologists and one dermatologist without prior knowledge about the

experimental procedures.

Western blotting

The wounds were resected 2 mm outside of the epithelial margin with a sterile scissors, and the scab and epithelium were eliminated. Normal skin was cut with a sterile disposable punch (diameter, 6 mm), and the epidermis was removed in similar manner. Fibroblasts derived from mice were collected in the 4th passage from the primary culture. Skin and fibroblast samples were homogenized and the lysates (20–40 μg) were electrophoresed in a 7.5% SDS-PAGE gel and transferred onto a polyvinylidene difluoride membrane. The membrane was immersed in blocking solution (Nacalai Tesque, Kyoto, Japan) for 20 minutes, and incubated overnight with primary antibodies diluted 1,000-fold. After the incubation of horseradish peroxidase-conjugated secondary antibodies, the immune complexes were visualized using Clarity Western ECL Substrate (Bio-Rad Laboratories, Hercules, CA, USA) according to the manufacturer's instructions.

Antibodies

The following antibodies (Abs) were used in this study: rabbit anti-mouse hPRDX4 mAb (Thermo Fisher Scientific, Waltham, MA, USA; PA3-753), mouse anti-human α-SMA

mAb (Dako Cytomation, Carpinteria, CA, USA; #M0851), 8-OHdG mAb (Japan Institute for the Control of Aging, Fukuroi, Japan; #bs-1278R), rat anti-mouse Ly-6G/Ly-6C (Gr-1) mAb Gr-1 (Southern Biotech, Birmingham, AL; #1900-31), rat anti-mouse Mac-2 mAb (Cedarlane Laboratories Ltd., Burlington, ON, CAN; #CL8942), rabbit anti-mouse CD3 pAb (Abcam, Cambridge, MA, USA; #ab5690), rabbit anti-mouse Ki-67 (Abcam; #ab16667), rat anti-mouse CD31 (Dianova GmbH, HAM, DEU; # DIA310), rabbit anti-mouse β-actin mAb (Cell Signaling, Danvers, MA, USA; #4970), rabbit anti-mouse TNF-α (D2D4) mAb, (Cell Signaling; #11948), mouse anti-mouse IL-1β (3A6) mAb (Cell Signaling; #12242), rabbit anti-mouse NF kappa B (D14E12) mAb (Cell Signaling; #4695), rabbit anti-mouse caspase3 (Cell Signaling; #9662), rabbit anti-mouse cleaved caspase3(Asp175) (5A1E) mAb (Cell Signaling; #9664), rabbit anti-mouse cyclin D1 (Cell Signaling; #2978), rabbit anti-mosue vimentin (D21H3) mAb (Cell Signaling; #5741), rabbit anti-mouse p38 MAPK (D13E1) mAb (Cell Signaling; #8690), rabbit anti-mouse phospho p38 MAPK (Thr180/Tyr182) mAb (Cell Signaling; #4511), rabbit anti-mouse p44/42 MAPK (Erk1/2) mAb (Cell Signaling; #4695), rabbit anti-mouse phospho p44/42 MAPK (Erk1/2) (Thr202/Tyr204) mAb (Cell Signaling; #4370), rabbit anti-mouse MEK1/2 mAb (Cell Signaling; #9122), rabbit anti-mouse phospho MEK1/2 (Ser217/221) mAb (Cell Signaling; #9121), rabbit anti-mouse cFOS (9F6) mAb (Cell

Signaling; #2250), rabbit anti-mouse phospho cFOS (Ser32) (D82C12) mAb (Cell Signaling; #5348), mouse anti-human FGF basic mAb (Abcam; #ab181), rabbit anti-mouse TGF-β mAb (Abcam; #ab92486), rabbit anti-mouse PDGF-BB mAb (Thermo Fisher Scientific; #PA5-19524), Alexa Fluor™ 594 donkey anti-rabbit IgG (Thermo Fisher Scientific, #A21207).

The ELISA to detect growth factor in serum

The serum FGF2, PDGF-BB and TGF-β1 levels were measured at 7 days after injury using a Quantikine ELISA KIT (# MFB00, # MBB00, # SB100B, respectively. R & D systems, Minneapolis, MN, USA). The results are shown as a mass per milliliter.

Measurement of the TBARS levels in serum and fibroblast lysates

We measured the serum and fibroblast oxidative stress levels using a thiobarbituric acid reactive substance (TBARS) Assay Kit (Cayman Chemical Company, Ann Arbor, MI) according to the manufacturer's instructions. Serum collected 7 days after injury was used. Fibroblasts were lysed with an ultrasonic homogenizer before the analysis. The results from serum samples are expressed as the molar concentration of malondialdehyde (MDA), while those from fibroblasts lysates are shown as picomoles of MDA per 1×10^6 cells.

Measurement of hydrogen peroxide in serum and fibroblast lysates

Serum collected at 7 days after injury and fibroblast lysates were used. We used a hydrogen peroxide colorimetric detection kit (Enzo Life Sciences, Farmingdale, NY, USA) according to the manufacturer's instructions. Results from serum and fibroblast lysates were expressed as nanograms of hydrogen peroxide per milliliter or per 1×10^6 cells respectively.

RNA Extraction and Quantitative Real-time RT-PCR

Total RNA was extracted from normal tissue and wound tissue using a Relia Prep™ RNA Tissue Miniprep kit (Promega, Leiden, Netherlands; #Z6112), and first-strand cDNA was synthesized using a High Capacity RNA-to-cDNA kit (Thermo Fischer Scientific, #4387406) according to the manufacturers' instructions. Quantitative real-time PCR was performed in a volume of 20 µL using gene-specific primers and EagleTaq Universal Master Mix (Nippon Genetics, Tokyo, Japan, #07260296190) in a QuantStudio™ 12K Flex Real-Time PCR System (Thermo Fisher Scientific, #4472380). Each sample was analyzed in triplicate in separate wells for COL1A1, COL3A1, and ribosomal 18S genes. The average of three threshold cycle values for

the target and 18S genes were calculated, and then analyzed using the comparative Ct method. The custom-made primers and TaqMan probes for COL1A1 (Assay ID: Mm01254476) and COL3A1 (Mn00801666) gene amplification were purchased from Life Technologies (Life Technologies, Carlsbad, CA, USA).

Cell culture

Skin fibroblasts were isolated from male WT and Tg mice at four weeks of age. To culture fibroblasts, a 1×1-cm piece of full thickness skin was cut from the dorsum of a euthanized mouse after hair removal. The skin was then washed three times in PBS containing 1% penicillin and 1% streptomycin, and the subcutaneous fat tissue was removed with a sterile blade under sterile conditions. The skin was cut into approximately 1-mm square small pieces, and each piece was placed on a 10-cm culture dish with the dermis facing down. Small drops of DMEM containing 10% FBS were placed on each piece of skin, the sample was incubated at 37°C under 5% CO_2 for one hour. Next, 8 ml of DMEM containing 10% FBS, 1% penicillin and 1% streptomycin was injected extremely slowly onto the dish, to avoid detachment of the pieces from the dish surface. Approximately 10 days later, the fibroblasts migrated out of the skin and adhered to the dish surface. The fibroblasts were cultured in DMEM containing 10% FBS, and passaged just before they

formed confluent monolayers.

Cell Counting Kit-8 proliferation assay

Mouse skin-derived fibroblasts in each generation were seeded in 96-well plates at a density of 5×10^3 cells per well. Five replicate wells were used per group. Cell viability was measured at 0, 24, 48, and 72 hours after seeding using a cell counting Kit-8 (CCK8, Dojindo Molecular Technologies, Tokyo, Japan) according to the manufacturer's instructions. The reproducibility of this study was confirmed by three repeated experiments.

Cell migration assay

A suspension of 5×10^4 fibroblasts were applied to 8-mm pore inserts (Corning Incorporated), with serum-free media in the upper chamber and 10% fetal bovine serum in the lower chamber. After 6 hours of culturing, the migrated cells were fixed by methanol and stained with 4', 6-diamidino-2-phenylindole (DAPI (Abbott Laboratories, Abbott Park, IL, USA; #6J4901)). Three replicate wells were used per group and this assay was repeated in triplicate. Migrated cells were counted at 100× magnification using the Image J software program.

Exposure of cells to H_2O_2

Mouse-derived fibroblasts from young mice, at the 4th passage, were seeded in a 96-well plate (1×10^4 cells / well) and cultured in plain DMEM for 6 h at 37°C. Cells were treated with DMEM containing 2.5, 5 and 10 μM H_2O_2 for 24 hours later, cell viability—expressed as the percentage of normal control—was measured. Cell viability was measured using a Cell Counting Kit-8 (as described above). n=5 for each concentration in each experiment, and each experiment was repeated 3 times.

Immunofluorescence staining

Primary cells of dermal fibroblasts were rinsed with phosphate-buffered saline (PBS) and immediately fixed in 10% neutral-buffered formalin at room temperature for 30 minutes. The frozen sections of healing skin tissue and primary cells of dermal fibroblasts were rinsed with phosphate-buffered saline (PBS) and immediately fixed in 4% paraformaldehyde in 0.1 M PBS at pH 7.4 at room temperature. Cells were incubated with anti-hPRDX4 mAb (1:1000, Thermo Fisher Scientific) for 1 hour, then incubated with secondary antibodies (1:1000, Thermo Fisher Scientific) for 30 minutes under shading and counterstained with DAPI (Abbott Laboratories) in the mounting media. All

images were captured with a BIOREVO BZ-9000 fluorescence microscope (KEYENCE, Osaka, Japan).

Statistical analysis

Data were expressed as the mean ± standard error of the mean (SEM). An unpaired Student's *t*-test was performed to compare values between two groups. *P* values of <0.05 were considered to indicate statistical significance. All statistical analyses were performed using the JSTAT software program (made by Dr. Sato Masato).

Supplementary References:

Chen B, Kao HK, Dong Z, Jiang Z, Guo L. Complementary Effects of Negative-Pressure Wound Therapy and Pulsed Radiofrequency Energy on Cutaneous Wound Healing in Diabetic Mice. Plast Reconstr Surg. 2017;139:105-17.

Guo X, Noguchi H, Ishii N, Homma T, Hamada T, Hiraki T, et al. The Association of Peroxiredoxin 4 with the Initiation and Progression of Hepatocellular Carcinoma. Antioxid Redox Signal 2019;30:1271-84.

Guo X, Yamada S, Tanimoto A, Ding Y, Wang KY, Shimajiri S, et al. Overexpression of peroxiredoxin 4 attenuates atherosclerosis in apolipoprotein E-knockout mice. Antioxid Redox Signal 2012;17:1362-75.

Iuchi Y, Okada F, Tsunoda S, Kibe N, Shirasawa N, Ikawa M, et al. Peroxiredoxin 4 knockout results in elevated spermatogenic cell death via oxidative stress. Biochem J 2009;419:149–58.

Meier JL and StinskiMF. Regulation of human cytomegalovirus immediate-early gene expression. Intervirology 1996;39:331–42.

Shirakata Y, Kimura R, Nanba D, Iwamoto R, Tokumaru S, Morimoto C, et al. Heparin-binding EGF-like growth factor accelerates keratinocyte migration and skin wound healing. J Cell Sci. 2005;118:2363-70.

Yamada S, Ding Y, Sasaguri Y. Peroxiredoxin 4: critical roles in inflammatory diseases. J UOEH 2012;34:27–39.